# Oxidative Modification of a Carboxyl-Terminal Vicinal Methionine in Calmodulin by Hydrogen Peroxide Inhibits Calmodulin-Dependent Activation of the Plasma Membrane Ca-ATPase†

Yihong Yao,‡ Danhong Yin,‡ Gouri S. Jas,§ Krzysztof Kuczera,‡,§ Todd D. Williams,|| Christian Schöneich,⊥ and Thomas C. Squier*,‡

*Departments of Biochemistry, Chemistry, and Pharmaceutical Chemistry and Mass Spectrometry Laboratory, University of Kansas, Lawrence, Kansas 66045-2106*

*Received July 25, 1995; Revised Manuscript Received November 22, 1995*⊗

ABSTRACT: In order to investigate the possibility that calmodulin (CaM) may be a principal target of reactive oxygen species (ROS) produced under conditions of oxidative stress, we have examined wheat germ CaM for the presence of highly reactive sites that correlate with the loss of function. Using reversed-phase HPLC and FAB mass spectrometry after proteolytic digestion, we have identified the sites of modification by hydrogen peroxide. We find that one of the vicinal methionines (i.e., $Met_{146}$ or $Met_{147}$) near the C-terminus of CaM is selectively oxidized. The ability of CaM to bind and to activate the plasma membrane (PM)-Ca-ATPase from erythrocytes was measured. There is a 30-fold decrease in the calcium affinity of oxidatively modified CaM. While there is little change in the binding constant between the carboxyl-terminal domain of calcium-saturated CaM and a peptide homologous to the autoinhibitory sequence of the PM-Ca-ATPase, we find that there is a 9-fold reduction in the affinity of the amino-terminal domain of CaM with respect to the ability to bind target peptides. The extent of oxidative modification to one of the vicinal methionines near the carboxyl-terminal domain correlates with the loss of CaM-dependent activation of the PM-Ca-ATPase. The presence of oxidatively modified CaM prevents native CaM from activating the PM-Ca-ATPase, indicating that the oxidatively modified CaM binds to the autoinhibitory sequence on the Ca-ATPase in an altered nonproductive conformation. We suggest that the functional sensitivity of CaM to the oxidation of one of the C-terminal vicinal methionines permits CaM to serve a regulatory role in modulating cellular metabolism under conditions of oxidative stress. The predominant oxidation of a methionine near the carboxyl terminal of CaM is rationalized in terms of the enhanced solvent accessibility of these vicinal methionines.

A growing body of literature suggests that oxidative stress and the associated production of reactive oxygen species (ROS)[1] are normal consequences of oxidative metabolism, primary factors associated with aging and a range of degenerative and debilitating diseases, and are identified with the loss of calcium regulation that often precedes cellular death (Harman, 1987; Nicotera et al., 1991; Kukreja & Hess, 1992, 1994; Coyle & Puttfarcken, 1993; Rosen et al., 1993). It is now clear that cellular proteins are susceptible to ROS, and that the selective modification of amino acids in the active site of proteins can have a significant impact on cellular function [reviewed by Stadtman (1992, 1993)]. However, there are currently limited examples in which the oxidative modification of specific amino acids and the associated functional consequences have been identified in functionally relevant calcium-regulatory proteins.

In order to mechanistically understand the observed relationships between oxidative stress, the production of ROS, and the rise in intracellular calcium levels we have focused our attention on two of the major proteins involved in both calcium signaling and calcium homeostasis in all cells, i.e., calmodulin (CaM) and the plasma membrane (PM)-Ca-ATPase. The latter protein is activated by CaM to maintain the low intracellular calcium concentrations

† Supported by the American Heart Association (Grant 1697) and the National Institutes of Health (NIH) (Grant AG12993). G.S.J. was supported by a postdoctoral fellowship from the American Heart Association (KS-95-F-7). The frequency-domain fluorometer was purchased with the aid of NIH Grant GM46837 and National Science Foundation Grant BIR-9116212, and by the University of Kansas. The tandem mass spectrometer was purchased with the aid of NIH Grant S10 RR0 6294 and by the University of Kansas.

* Correspondence should be addressed to this author. Telephone: (913)-864-4008. FAX: (913)-864-5321. E-mail: TCSQUIER@KUHUB.CC.UKANS.EDU.

‡ Department of Biochemistry.

§ Department of Chemistry.

|| Mass Spectrometry Laboratory.

⊥ Department of Pharmaceutical Chemistry.

⊗ Abstract published in *Advance ACS Abstracts,* February 15, 1996.

[1] Abbreviations: amu, atomic mass unit; CaM, calmodulin; C25W, a peptide homologous to the CaM binding sequence on the autoinhibitory domain of the plasma membrane Ca-ATPase whose sequence is QILWFRGLNRIQTQIRVVNAFRSSC; TPCK, L-(tosylamino)-2-phenylethyl chloromethyl ketone; DTT, dithiothreitol; EDTA, ethylenediaminetetraacetic acid; EGTA, ethylene glycol bis(β-aminoethyl ether)-*N*,*N*,*N*′,*N*′-tetraacetic acid; Endo GluC, endoproteinase GluC; F52, a peptide homologous to the CaM binding sequence on the autoinhibitory sequence of a MARCKS homolog whose sequence is KKKKKFSFKKPFKLSGLSFKRNRK; FAB-MS, fast atom bombardment mass spectrometry; FURA-2, 1-[2-(5-carboxyazol-2-yl)-6-aminobenzofuran-5-oxy]-2-(2-amino-5-methylphenoxy)ethane-*N*,*N*,*N*′,*N*′-tetraacetic acid; GnHCl, guanidine hydrochloride; HEPES, *N*-(2-hydroxyethyl)piperazine-*N*′-2-ethanesulfonic acid; HOMOPIPES, homopiperazine-*N*,*N*′-bis(2-ethanesulfonic acid); HPLC, high-performance liquid chromatography; Met, methionine; MetSO, methionine sulfoxide; PAGE, polyacrylamide gel electrophoresis; PM, *N*-(1-pyrenyl)maleimide; PM-Ca-ATPase, erythrocyte plasma membrane Ca-ATPase; ROS, reactive oxygen species; SDS, sodium dodecyl sulfate; TFA, trifluoroacetic acid.

0006-2960/96/0435-2767$12.00/0 

characteristic of healthy cells, and is functionally impaired during both normal cellular aging and ischemic damage (Carafoli, 1987, 1991; Falchetto et al., 1991; Michaelis, 1989; Michaelis et al., 1992). While the loss of calcium transport function has been suggested to involve ROS (Kukreja & Hess, 1992; Chaudière, 1994), it is unclear if the target of oxidative modification is the PM-Ca-ATPase or may involve its activator CaM. However, the decline in the maximal ATPase activity of the PM-Ca-ATPase observed in intact human red cells associated with aging can be reversed subsequent to purification of the erythrocyte ghosts and addition of exogenous CaM (Clark & Shohet, 1985; Clark, 1988), suggesting that CaM may be the principal target of ROS during normal aging. The emphasis of the current study with respect to the assessment of the sensitivity of CaM to oxidative damage is based upon both the physiological importance and amino acid composition of CaM (see below).

CaM is a ubiquitous and abundant (approximately 30 $\mu$M in brain) eukaryotic calcium binding protein found in all eukaryotic tissues, which functions in the regulation of a range of cellular processes, including muscle contraction, neurotransmission, neuronal plasticity, cytoskeletal assembly, and a host of reactions involved in the energy and biosynthetic metabolism of the cell [reviewed by Carafoli (1987) and Wylie and Vanaman (1988)]. CaM contains an exceptionally high content of methionine residues (eight in plants, nine in animals) that correspond to about 6% of the amino acids (4 times the average occurrence of this amino acid in most proteins). The high methionine content in CaM is related to the ability of CaM to activate a wide range of target proteins with variable binding sites (O'Neil et al., 1989; Gellman, 1991; Williams, 1992; Crivici & Ikura, 1995). In fact, the high-resolution structure of the calcium-liganded form of CaM in association with the autoregulatory sequence from both skeletal and smooth muscle myosin light chain kinase and calmodulin-dependent protein kinase demonstrates that essentially all methionines are involved in the interaction with target peptides, and methionine residues comprise nearly half of the binding surface (O'Neil & DeGrado, 1990; Meador et al., 1992, 1993; Ikura et al., 1992). Methionine is easily oxidized to the corresponding sulfoxide by a range of ROS with rate constants comparable, and sometimes higher than the comparable oxidation of cysteine in its protonated form. In addition, oxidation of the nonpolar thioether to the corresponding sulfoxide results in a dramatic increase in polarity (Gellman, 1991). Thus, the high content of methionine residues in CaM is likely to predispose this protein to oxidative modification in the cytosol. In support of this hypothesis, Fliss and Docherty (1987) identified significant levels of methionine oxidation in rat heart tissue and myocytes exposed to ROS generating systems, and have identified the calcium-regulating excitation−contraction system in ischemic heart tissue as a primary target for ROS.

In the present study, we have assessed the oxidative damage to wheat germ CaM by hydrogen peroxide, correlating oxidative modifications of specific amino acids with alterations in the structure and functional properties of CaM. Wheat germ CaM has 90% sequence identity to animal CaM and fully activates target proteins from animal sources (Strasburg et al., 1988; Yao et al., 1994). Wheat germ CaM was used in the present study due to its unique amino acid composition. The single pair of vicinal methionines simplifies the analysis of the functional relationships between specific sites of oxidative modification and function. The single tyrosine in the carboxyl-terminal domain (i.e., $Tyr_{139}$) enables us to use the associated fluorescence signal to monitor protein structural changes associated with calcium binding site IV. The unique cysteine (i.e., $Cys_{27}$) in the amino-terminal domain (Figure 1) allows the covalent attachment of a fluorophore (i.e., pyrenylmaleimide), as previously described to selectively monitor conformational changes associated with calcium binding to site I. Together, these unique fluorescent reporter groups permit the monitoring of the conformational coupling between the opposing globular domains, and measurement of the binding affinity of CaM to target peptides (Yao et al., 1994). The functional relevance of oxidative modification was measured with respect to the ability of CaM to activate the PM-Ca-ATPase, permitting us to assess possible relationships between the oxidative modification of CaM and the loss of calcium regulation associated with conditions of oxidative stress (including aging). Correlations between the oxidative modification of defined sequences within CaM, structural changes associated with calcium activation, and the subsequent binding to peptides that are homologous to the autoinhibitory domain of the PM-Ca-ATPase are discussed in terms of the possible regulation of cellular metabolism by ROS.

## EXPERIMENTAL PROCEDURES

*Materials.* Hydrogen peroxide ($H_2O_2$) was obtained from Fisher (Pittsburgh, PA). *N*-(1-Pyrenyl)maleimide (PM) and 1-[2]-(5-carboxyoxazol-2-yl)-6-aminobenzofuran-5-yl-2-(2-amino-5-methylphenoxy)ethane-*N*,*N*,*N*′,*N*′-tetraacetic acid) (FURA-2) were obtained from Molecular Probes, Inc. (Juntion City, OR). Trifluoroacetic acid (TFA) was obtained from Aldrich (Milwaukee, WI). Type XIII TPCK-treated trypsin and type I-S soybean trypsin inhibitor were obtained from Sigma (St. Louis, MO). Endoproteinase Glu-C from *Staphylococcus aureus V8* was obtained from Boehringer Mannheim (Indianapolis, IN). $^{45}CaCl_2$ was obtained from ICN (Costa Mesa, CA). All other chemicals were the purest grade commercially available. CaM was purified from wheat germ using the procedure outlined by Strasburg et al. (1988), and purity was assessed by both SDS−PAGE and HPLC. Porcine erythrocyte ghosts were prepared essentially as described by Niggli et al. (1979). Purified wheat germ CaM and ghosts were stored at −70 °C. CaM binding peptide C25W (QILWFRGLNRIQTQIRVVNAFRSSC) was synthesized and purified by HPLC by the Biotechnology and Microchemical Core Facility at Kansas State University. CaM binding peptide F52 (KKKKKFSFKKPFKLSGLSFKRNRK) was kindly provided by J. David Johnson (Ohio State).

*Specific Derivatization of $Cys_{27}$ in CaM with PM.* The chemical modification of $Cys_{27}$ was carried out essentially as described in Yao et al. (1994), where the specificity of labeling the single cysteine in wheat germ CaM was described in detail. The extent of label incorporation was determined using the molar extinction coefficient for PM ($\epsilon_{343}$ = 36 000 $M^{-1}$ $cm^{-1}$). In all cases, derivatization of native or oxidatively modified CaM with PM resulted in the quantitative labeling of $Cys_{27}$ such that greater than 90% of the site was modified, irrespective of whether labeling was carried out using native or oxidatively modified CaM. Prior to chemical derivatization, CaM was first dissolved in 6 M GnHCl, 25 mM HEPES (pH 7.5), 50 mM DTT, and 1 mM

EDTA buffer and incubated at 25 °C for 2 h in order to eliminate intermolecular cross-linking. DTT was removed by dialysis against deionized water prior to lyophilization. CaM concentration was determined using the micro BCA assay (Pierce, Rockford, IL), using a stock solution of desalted bovine CaM as a standard, whose concentration was determined using the published extinction coefficient for bovine CaM ($\epsilon_{277} = 3029$ $M^{-1}$ $cm^{-1}$ in the presence of 0.1 mM $CaCl_2$; Klee & Vanaman, 1982; Strasburg et al., 1988). The apparent extinction coefficient for desalted wheat germ CaM in the presence of 0.1 mM $CaCl_2$ was therefore determined to be $\epsilon_{277} = 1565$ $M^{-1}$ $cm^{-1}$, and is consistent with the presence of a single tyrosine (bovine CaM has two tyrosines), the observed modification of $0.98 \pm 0.05$ cysteine per CaM with DTNB, and the calcium binding stoichiometry of $4.07 \pm 0.05$ calciums bound per CaM (see below).

*Oxidative Modification of Methionine within CaM.* 60 $\mu$M CaM (1.0 mg/mL) was dissolved in 50 mM HOMOPIPES, 0.1 M KCl, 1 mM $MgCl_2$, and 0.1 mM $CaCl_2$ at pH 5.0. $H_2O_2$ was added to make the final concentration 5 mM, where the concentration of $H_2O_2$ was determined using the extinction coefficient at 240 nm ($\epsilon_{240} = 39.4 \pm 0.2$ $M^{-1}$ $cm^{-1}$; Nelson & Kiesow, 1972). Under these conditions, methionines are predicted to be selectively oxidized to their corresponding sulfoxide (Vogt, 1995). The oxidation was carried out at 25 °C. At different time intervals, the reaction was terminated by applying the sample onto a Sephadex G-25 column (1.6 × 23 cm), and CaM was separated from the unreacted $H_2O_2$ and was subsequently lyophilized.

*Enzymatic Assay.* The Ca-ATPase activity of erythrocyte ghosts was determined using the methods described by Lanzetta et al. (1979) for measuring phosphate release. The ghost membrane protein concentration was determined by the method of Biuret (Gornal et al., 1949). When applicable, the free calcium concentration was calculated using a modified version of the computer program previously described (Fabiato & Fabiato, 1979; Fabiato, 1988), which calculates the multiple equilibria between all ligands in solution. The free calcium concentration was confirmed using 1-[2-(5-carboxyazol-2-yl)-6-aminobenzofuran-5-oxy]-2-(2-amino-5-methylphenoxy)ethane-*N*,*N*,*N*′,*N*′-tetraacetic acid (FURA-2; $\lambda_{ex} = 340$ nm; $\lambda_{em} = 510$ nm), as described previously (Yao et al., 1994). In all cases, we find an apparent dissociation constant of $80 \pm 5$ nM, in close agreement with the literature value [$K_D \approx 0.1$ $\mu$M (Haugland, 1992)].

*Equilibrium Dialysis.* The stoichiometry of calcium binding to CaM was determined using 0.2 mM $^{45}CaCl_2$ (10 000 cpm/nmol) that was equilibrated with 30 $\mu$M CaM (0.5 mg/mL) in a buffer containing 0.1 M KCl, 1 mM $MgCl_2$, and 100 mM HEPES (pH 7.5) essentially as previously described (Burgess et al., 1980).

*Identification of Proteolytic Fragments.* In order to assess sites associated with oxidative modification, CaM (60 $\mu$M) was subjected to exhaustive tryptic digestion (0.6 $\mu$M trypsin in 50 mM potassium phosphate at pH 8.0 for 9 h at 37 °C). Digestion was stopped upon addition of 1.8 $\mu$M trypsin inhibitor. Alternatively, CaM (120 $\mu$M) was digested with endoproteinase Glu-C (0.2 mg/mL) in 50 mM sodium phosphate at pH 7.8 for 12 h at 37 °C. Proteolytic fragments were separated on HPLC using a Vydac C4 reverse-phase column employing a linear gradient varying from 0.1% TFA to 0.1% TFA in 80% acetonitrile/20% water at a rate of 1% per minute, essentially as described previously (Ota & Clark, 1989). The respective peaks were monitored at 214 nm. The detected peaks were pooled, lyophilized, and subjected to fast atom bombardment (FAB) mass spectrometry. Mass spectra were obtained on an AUTOSPEC-Q tandem hybrid mass spectrometer (VG Analytical Ltd., Manchester, U.K.) equipped with an OPUS data system. FAB mass spectrometry experiments were performed using a cesium gun operated at 20 keV energy and 2 $\mu$A emission. Sample solutions in $CH_3CN/H_2O$ (1:1) were added to thioglycerol/glycerol (1:1) as the matrix. Peptide esterifications were carried out by dissolving dried peptide fractions in 0.2 N acetyl chloride in hexanol and warming at 35 °C for 1 h. The hexanol peptide solutions were analyzed directly. Mass identification was assisted through the use of software (GPMAW from Lighthouse data, Aalokken 14, DK-5250, Odense SV, Denmark) that permits the identification of all possible combinations resulting from proteolytic digestion that are consistent with an experimental mass, and facilitates peak identification through the prediction of the elution profile of individual peptides based on an average hydrophobicity index (Kyte & Doolittle, 1982).

*Calculation of Free CaM Concentrations.* The concentration of free CaM was obtained from the relationship:

$$[\mathrm{CaM}]_{\mathrm{free}} = [\mathrm{CaM}]_{\mathrm{total}} - (V_{\mathrm{max}} - V)[\mathrm{CaM}]_{\mathrm{max}} \quad (1)$$

where $V_{max}$ is the maximal calmodulin-dependent ATPase activity, $V$ is the observed ATPase activity at a defined concentration of CaM, $[CaM]_{free}$ is the concentration of CaM free in solution, $[CaM]_{total}$ is the total concentration of CaM added to the solution, and $[CaM]_{max}$ is the total binding capacity of the erythrocyte ghosts for CaM, which was estimated to correspond to 18 pmol of CaM bound per milligram of erythrocyte ghost. The latter number is in good agreement with earlier evidence that indicates that (i) the PM-Ca-ATPase represents virtually the only CaM binding protein in the purified inside-out erythrocyte ghosts used in this study, (ii) one CaM binds to every two PM-Ca-ATPase molecules, and (iii) the PM-Ca-ATPase represents about 0.5% (w/w) of the total membrane protein in porcine erythrocyte ghosts [Hinds & Andreasen, 1981; Cavieres, 1984; Kosk-Kosicka et al., 1990; Vorherr et al., 1991; reviewed by Carafoli (1987)].

*Fluorescence Spectroscopy Measurements.* Steady-state fluorescence intensities and time-resolved fluorescence lifetimes were measured using an ISS K2 fluorometer, as described in detail (Yao et al., 1994). Excitation was at 351 nm for pyrenylmaleimide-labeled CaM and at 275 nm for tyrosine, using a Coherent Innova 400 laser with extended ultraviolet capabilities. Spectra were acquired with a Jovin Yvon monochromator with a single grating using 4 nm slits. Unless otherwise specified, the fluorescence emission of pyrene was collected using a Schott GG400 long-pass filter, and in the case of tyrosine, the fluorescence emission was collected using an Oriel band-pass filter centered at 320 nm (full-width half-maximum is 10 nm). All necessary corrections were made for the contribution of the observed steady-state signal intensity originating from Raman scattering (Yao et al., 1994). In all cases, the sample temperature was maintained at 25 °C.

*Decays of Fluorescence Intensity.* As described in detail (Yao et al., 1994), the fluorescence decays of pyrenylmale-

imide and tyrosine were fit using the method of nonlinear least squares to a sum of exponential decays (Bevington, 1969):

$$I(t) = \sum_{i=1}^{N} \alpha_i e^{-t/\tau_i} \quad (2)$$

where $\alpha_i$ are the preexponential factors, $\tau_i$ are the excited state decay times, and $N$ is the number of exponential components required to describe the decay. Subsequent to the measurement of the intensity decay, one can calculate the average lifetime, $\bar{\tau}$, which is weighted by the amplitudes associated with each of the preexponential terms, where

$$\bar{\tau} \equiv \sum_i \alpha_i \tau_i \quad (3)$$

and $\bar{\tau}$ is directly related to the average time the fluorophore is in the excited state. The amplitude weighting implies a direct relationship between $\bar{\tau}$ and the quantum yield of the fluorophore (Luedtke et al., 1981). Errors in the average lifetime are propagated, as described in Bevington (1969):

$$\frac{\sigma_{\bar{\tau}}^2}{\bar{\tau}^2} = \sum_i \left[ \frac{\sigma_{\alpha_i}^2}{\alpha_i^2} + \frac{\sigma_{\tau_i}^2}{\tau_i^2} \right] \quad (4)$$

where $\sigma_{\alpha_i}$ and $\sigma_{\tau_i}$ represent the standard errors associated with the amplitudes and lifetimes resolved from the fluorescence intensity decay, and were determined from a consideration of the $\chi^2$ surface of each parameter, as previously described (Johnson & Faunt, 1992; Yao et al., 1994).

*Calculation of Solvent Accessibility.* The structure of wheat germ CaM was modeled using the published coordinates for the crystal structures of human CaM (PDB File 1cLL; Chattopadhyaya et al., 1992) and paramecium CaM (PDB File 1osa; Rao et al., 1993) available from the Brookhaven Protein Data Bank, using the Protein Design module of the QUANTA modeling package (Molecular Simulations, Inc.). Subsequent to energy minimization with isotropic harmonic constraints using the CHARMM program (Bruccoleri & Karplus, 1986), the relative solvent accessibilities of the individual methionines in these structures were calculated relative to the exposed surface area to water, which was modeled as a sphere with a radius of 1.6 Å. The solvent accessibility of Met in CaM was compared with a small dipeptide (Gly-Met) and free sulfur, where the exposed surface area of sulfur is 44.1 and 50.2 Å$^2$, respectively.

*Calculation of Model-Dependent Fitting Parameters.* In order to quantitate the effect of oxidative modification at selective sites on CaM with respect to calcium activation, the binding of target proteins, and the activation of the PM-Ca-ATPase, we have fit our data to standard models involving the binding and activation of proteins involving one, two, or three binding sites, as discussed in detail elsewhere (Matthews, 1993; Pedigo & Shea, 1995). Therefore, if one assumes that there is a homogeneous population of independent ligand binding sites, then a titration of binding (or enzyme activation) can be fit to the equation:

$$Y = \frac{K_1[\mathrm{X}]_{\mathrm{free}}}{1 + K_1[\mathrm{X}]_{\mathrm{free}}} \quad (5)$$

where $Y$ in general represents the fraction of sites occupied with respect to a binding isotherm, $K_1$ represents the intrinsic association constant, and $[\mathrm{X}]_{\mathrm{free}}$ is the concentration of the unbound ligand, which corresponds to either the free calcium or the CaM concentration. In the case of enzyme activation, $Y$ represents the fraction of sites occupied that result in enzyme activation.

In the case of multiple ligand binding sites, one can explicitly analyze for the relative affinities and cooperative interactions between the individual ligand binding sites:

$$Y = \frac{K_1[\mathrm{X}]_{\mathrm{free}} + 2K_2[\mathrm{X}]_{\mathrm{free}}^2}{2(1 + K_1[\mathrm{X}]_{\mathrm{free}} + K_2[\mathrm{X}]_{\mathrm{free}}^2)} \quad (6)$$

where the macroscopic equilibrium constant $K_1$ corresponds to the sum of the intrinsic equilibrium constants ($k_1$ and $k_2$) associated with ligand binding to the two classes of binding sites and $K_2$ represents the intrinsic equilibrium constant for binding ligand to both classes of ligand binding sites ($k_1k_2k_{12}$). This provides a quantitative estimate of the lower limit with respect to the cooperative interactions between the sites (i.e., $k_{12}$; Pedigo & Shea, 1995). An analogous expression useful with respect to the analysis of peptide binding to CaM is the equivalent Scatchard form of the binding equation (Matthews, 1993):

$$[\mathrm{peptide}]_{\mathrm{bound}} = \left[ \frac{K_2[\mathrm{peptide}]_{\mathrm{free}} + 1}{1 + K_1[\mathrm{peptide}]_{\mathrm{free}} + K_1K_2[\mathrm{peptide}]_{\mathrm{free}}^2} \right] \times \text{maximal binding} \quad (7)$$

In this equation, $K_1$ and $K_2$ represent the association constants for each domain on CaM with respect to its association with target peptides. Peptide binding curves were measured using the fluorescence changes associated with either PM located at $Cys_{27}$ or the intrinsic probes located in calcium binding site IV on CaM (i.e., $Tyr_{139}$) or on the target peptide C25W (i.e., $Trp_4$). Assuming that one peptide binds to one CaM [reviewed by Crivici and Ikura (1995)] and that the observed fluorescence changes were linearly related to the concentration of bound peptide, then:

$$[\mathrm{peptide}]_{\mathrm{bound}} = \left[ \frac{|(F - F_0)|}{|(F_{\max} - F_0)|} \right] [\mathrm{CaM}]_{\mathrm{total}} \quad (8)$$

where $F_0$ is the initial fluorescence, $F_{\max}$ is the fluorescence observed in the presence of saturating concentrations of peptide, and $F$ is the observed fluorescence at a particular CaM concentration. $[\mathrm{CaM}]_{\mathrm{total}}$ is the total concentration of CaM in solution, and $[\mathrm{peptide}]_{\mathrm{bound}}$ is the concentration of peptide that is associated with CaM. Knowing $[\mathrm{peptide}]_{\mathrm{bound}}$, it is possible to calculate the concentration of peptide free in solution (i.e., $[\mathrm{peptide}]_{\mathrm{free}}$), where

$$[\mathrm{peptide}]_{\mathrm{free}} = [\mathrm{peptide}]_{\mathrm{total}} - [\mathrm{peptide}]_{\mathrm{bound}} \quad (9)$$

In order to fit our data to relevant equations relating to the calcium and peptide binding affinity of native and oxidatively modified CaM, we used the Levenberg−Marquardt algorithm contained in the programs ORIGIN (Microcal Software, Inc., Northampton, MA) and Mathcad (MathSoft Inc., Cambridge, MA) to extract free energy

parameters relating to the properties of the native and oxidatively modified CaM (Press et al., 1988). In the latter case, we were able to enhance the certainty of the calculated constants by simultaneously fitting a complete data set (containing five samples) obtained from CaM that contained variable degrees of oxidative modification to a two-state model, where

$$F(X) = \sum_i [\alpha_i Y_{\mathrm{CaM}_{\mathrm{native}}} + (1 - \alpha_i) Y_{\mathrm{CaM}_{\mathrm{oxidized}}}]\mathrm{span} + \mathrm{minimum} \quad (10)$$

The associated amplitudes for native ($\alpha_i$) and oxidatively modified ($1 - \alpha_i$ ) CaM are taken to be representative of the populations of native-like and structurally modified CaM. Span represents the dynamic range of the dependent variable, and minimum represents the value of the dependent variable at low ligand concentration. The association constants obtained for native CaM alone are used to fix $Y(\mathrm{CaM})_{\mathrm{native}}$, permitting a quantitative assessment relating to the properties of the oxidatively modified CaM species. The associated errors of the recovered parameters were obtained from a consideration of the error surfaces using the *F*-statistic, where the parameter of interest was systematically varied and all other parameters were floated to quantitatively consider possible cross-correlations between the calculated parameters (Johnson & Faunt, 1992). In the case of nonsymmetric error surfaces, the indicated uncertainty corresponds to the maximal deviation and is tabulated as the variance of the measurement. The significance of observed differences in the association constants between native and oxidatively modified CaM (see below) was calculated using the Students *t*-test using $P < 0.05$ to define a 95% confidence level.

In the presence of oxidatively modified CaM, one observes a decreased maximal velocity of the PM-Ca-ATPase that suggests that oxidatively modified CaM acts as a noncompetitive inhibitor of the PM-Ca-ATPase (see Results). In order to quantify this effect, we made use of the equation (Matthews, 1993):

$$\frac{\mathrm{ATPase}}{\mathrm{ATPase}_{\mathrm{max}}} = \frac{[\mathrm{CaM}]_{\mathrm{native}}}{(1/K_{\mathrm{a}})(1 + K_{\mathrm{I}}[\mathrm{CaM}]_{\mathrm{ox}}) + [\mathrm{CaM}]_{\mathrm{native}}(1 + K_{\mathrm{I}}[\mathrm{CaM}]_{\mathrm{ox}})} \quad (11)$$

where ATPase is the observed CaM-dependent ATPase activity at a particular concentration of CaM, $\mathrm{ATPase}_{\mathrm{max}}$ is the maximal observed calmodulin-dependent ATPase activity at saturating concentrations of CaM, $[\mathrm{CaM}]_{\mathrm{native}}$ and $[\mathrm{CaM}]_{\mathrm{ox}}$ are the relative concentrations of native and oxidatively modified CaM, $K_{\mathrm{a}}$ is the association constant for native CaM binding to the PM-Ca-ATPase, and $K_{\mathrm{I}}$ is the association constant for oxidatively modified CaM binding to the PM-Ca-ATPase. In this analysis, $K_{\mathrm{a}}$ is obtained from a consideration of native CaM in the absence of oxidatively modified CaM, and in order to account for the variable degree of oxidative modification, we consider the relative concentration of native and oxidatively modified CaM whose tertiary structure has been modified so as to alter the parameter of interest to represent a variable for each experiment, such that:

$$[\mathrm{CaM}]_{\mathrm{native}} = \alpha[\mathrm{CaM}]_{\mathrm{total}} \quad (12)$$

and

$$[\mathrm{CaM}]_{\mathrm{ox}} = (1 - \alpha)[\mathrm{CaM}]_{\mathrm{total}} \quad (13)$$

where $\alpha$ represents the fractional population of CaM with native-like structure, and $\alpha \leq 1.0$.

## RESULTS

*Oxidation of CaM by $H_2O_2$.* It has been suggested that some proteins contain specific amino acids that are prone to oxidation, and selectively inhibit activity (Stadtman, 1993). We wish to establish whether CaM might be selectively oxidized by ROS. Therefore, it is necessary to first define oxidatively sensitive sites, and then (see below) assess whether these sites are functionally significant. In view of the oxidative sensitivity of methionine and their important functional role in defining target protein binding sites in CaM [Gellman, 1991; Williams, 1992; Meador et al., 1992, 1993; Ikura et al., 1992; Vogt, 1995; reviewed by Crivici and Ikura (1995)], our strategy was to use oxidizing conditions that are as specific as possible for methionine (i.e., $H_2O_2$ at pH 5.0), in order to determine the relationship between specific sites of oxidative modification in the primary sequence and functional alterations in the protein. Therefore, CaM was exposed to 5.0 mM $H_2O_2$ for variable periods of time (i.e., 0, 1, 2, 4, and 10 h at 25 °C), and the structural and functional consequences of oxidative modification were determined. It should be noted that $H_2O_2$ selectively oxidizes methionine residues at acidic pH, whereas other amino acids such as tyrosine and cysteine may also be affected at physiological pH and higher (Vogt, 1995). The relative positions of the eight methionines found in plant CaM (which has 90% sequence *identity* and one additional amino acid relative to vertebrate CaM) within the primary sequence of wheat germ CaM are illustrated (Figure 1A), and their relative placement within the tertiary structure of calcium-saturated CaM is highlighted (Figure 1B). The positions of the individual methionines are designated relative to the peptide fragments generated subsequent to exhaustive tryptic digestion (Figure 1A; see below).

*Resolution of Tryptic Peptides by HPLC.* In order to define the positions of the modified amino acids in the primary sequence, we subjected CaM that had been exposed to $H_2O_2$ for various periods of time (see above) to exhaustive tryptic digestion and isolated the tryptic fragments of both the native and oxidized CaM using reversed-phase HPLC in order to identify their correspondence to the primary sequence of CaM (Figure 2). We were able to separate 11 major tryptic fragments from native (unoxidized) CaM, whose retention times on a C4 reversed-phase column vary between 15 and 50 min. Since the exhaustive digestion of CaM with trypsin is predicted to generate 12 major fragments containing 3 or more amino acids (Toda et al., 1985), it is clear that the majority of the tryptic fragments were resolved. The positions of the 8 methionines are depicted (Figure 1), and the associated tryptic fragments are numbered sequentially from the amino terminal of CaM relative to the 12 predicted tryptic fragments. Subsequent to the exposure of CaM to $H_2O_2$, we observe that the relative peak heights and areas of the vast majority of the tryptic fragments are unaffected, indicating that under these experimental condi-

A.

T1 T2 T3

ADQLTDEQNIAEFK↓EAFSLFDKDGDGC$_{27}$ITTK↓ELGTVM$_{97}$R↓

T4 T5+T6

SLGQNPTEAELQDM$_{52}$INEVDADGNGTIDFPEFLNLM$_{73}$AR↓KM$_{77}$K

T7+T8 T9 T10

↓DTDSEEELKEAFR↓VFDKDQDGFISAAELR↓HVM$_{110}$TNLGEKLT

T10$_{cont.}$ T11 T12

DEEVDEM$_{125}$IR↓EADVDGDGQINY$_{139}$EEFVK↓VM$_{146}$M$_{147}$AK

B

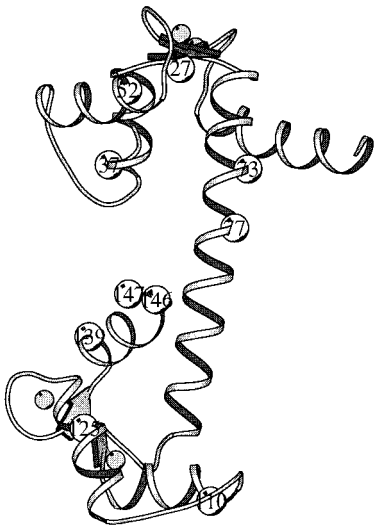


FIGURE 1: Positions of methionines within calmodulin. (A) Positions of the eight methionines within the primary structure of wheat germ CaM are illustrated to facilitate the direct comparison of the oxidative sensitivities of the various tryptic fragments presented in Figures 2 and 3. The positions of tryptic cleavage sites within the primary sequence of CaM are designated with vertical arrows, and the 12 fragments generated subsequent to tryptic cleavage are indicated by the letter T followed by a number. The tryptic fragments are numbered relative to the amino-terminal domain as previously described (Toda et al., 1985). $Cys_{27}$ and $Tyr_{139}$ represent sites associated with fluorescence signals, as described in the text. (B) The relative positions of all eight methionines within the tertiary structure of CaM are highlighted in the ribbon drawing of the backbone fold of the calcium-saturated form of CaM. The coordinates are taken from Brookhaven Protein Data Bank file 1cll.pdb (Chattopadhyaya et al., 1992), and the ribbon drawing was created using MolSript (Kraulis, 1991). Shaded circles represent calcium ligands. The model does not attempt to depict known alterations in the tertiary structure that occur in solution [Török et al., 1992; Yao et al., 1994; reviewed by Crivici and Ikura (1995)].

tions $H_2O_2$ modifies a limited number of amino acids. However, a reduction is observed in the relative areas of several peaks in the chromatogram obtained from the oxidized CaM relative to that observed in native CaM, with retention times of 17.4 min (T12), 23.7 min (T3), and the doublet of peaks at 49 min (T4), that is associated with the appearance of the corresponding oxidation products with retention times of 11.8 min [T12(SO)], 18.9 min [T3(SO)], a doublet of peaks at 43 min [$T4(SO)_2$], and a doublet of peaks at 46 min [T4(SO)]. The relationship between the parent peaks and their corresponding oxidation products was independently obtained by the selective oxidation of specific tryptic fragments with $H_2O_2$, and these peptides were subsequently rechromatographed in order to determine the alteration in retention times associated with the oxidized products of the parent tryptic fragments (data not shown).

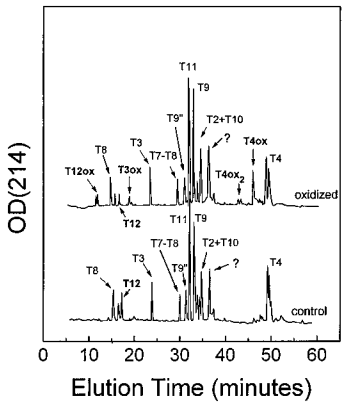


FIGURE 2: HPLC resolution of tryptic peptides following oxidation of calmodulin with $H_2O_2$. Two representative chromatograms are shown corresponding to the resolved peptides subsequent to exhaustive tryptic digestion (9 h, 37 °C) of control and oxidatively modified calmodulin. The oxidatively modified sample illustrated was obtained subsequent to incubation of CaM in the presence of 5 mM $H_2O_2$ for 10 h at pH 5.0. The assignments of the parent fragments and the corresponding sulfoxides are shown with respect to the 12 expected tryptic peptides, as described in Table 1. The amino-terminal fragment T1 ($Ala_1-Lys_{14}$) and the small tryptic fragments (i.e., T5 and T6) corresponding to $Lys_{76}-Lys_{78}$ are not observed in this digestion. Likewise, tryptic fragments T2 and T10 overlap and are not resolved from one another under these conditions. T7−T8 is a single peptide that was not cleaved at $Lys_{87}$. Peptides were separated on a Vydac C4 reversed-phase column employing a linear gradient varying from 0.1% TFA to 0.1% TFA in 80% acetonitrile/20% water at a rate of 1% per minute. The respective peaks were monitored at 214 nm. The detected peaks were pooled, lyophilized, and subjected to FAB-mass spectroscopy. The background absorbance from the solvent was digitally subtracted from both chromatograms.

This provides a quantitative identification of the relationship between parent peaks and their associated oxidative product (Figure 2). Under these experimental conditions, we are not able to resolve the two overlapping tryptic fragments with retention times of 34.6 min (T2 and T10). Therefore, it was necessary to define other experimental conditions to quantitatively measure the sensitivity of these peptides to oxidative modification (see below).

*Identification of Amino Acid Modifications in CaM by Positive FAB Mass Spectrometry.* The tryptic fragments separated by reversed-phase HPLC were identified using FAB mass spectrometry. In addition to recording the molecular masses of the individual peptide fragments, several fragments (e.g., T7−T8; Table 1) have been derivatized by esterification with hexan-1-ol in hydrochloric acid (Falick & Maltby, 1989). This method greatly enhances the mass spectrometric response factor for polar peptides and yields protonated molecular ions of masses ($M+H^+$) which are 84 mass units higher than the nonderivatized peptide for each derivatization site, and provides increased confidence with respect to the identification of the purified peptides obtained from the trypsin digestion of CaM. The masses of isolated peptides are compared to the expected theoretical masses of the tryptic fragments (Table 1). One observes that in all cases the experimentally observed mass is within 0.1% of the theoretical mass from that expected for the corresponding protonated peptide fragment. The identifications of T12, T3, and T4 are further confirmed by the correspondence between the loss of parent peaks upon oxidative modification, and the generation of oxidative products with the expected masses and retention times on HPLC chromatograms corresponding

Table 1: FAB Mass Spectroscopic Identification of Tryptic Fragments Isolated from Native and Oxidatively Modified Calmodulin[a]

| peak | $t_R$ (min) | sequence | derivatization with $C_6H_{13}OH$/HCl | $[M+H]^+_{theoretical}$[b] | $[M+H]^+_{experimental}$ |
|---|---|---|---|---|---|
| T12(SO)[d] | 11.8 | $V_{145}-(MO)-K_{149}$ | | 595.3 | 595.2 |
| T8 | 14.8 | $E_{88}-R_{91}$ | | 522.3 | 522.4 |
| T12 | 17.4 | $V_{145}-K_{149}$ | | 579.3 | 579.4 |
| T3(SO)[d] | 18.9 | $E_{32}-(MO)-R_{38}$ | | 821.4 | |
| T3 | 23.7 | $E_{32}-R_{38}$ | | 805.4 | 804.8 |
| T7 + T8 | 29.4 | $D_{79}-R_{91}$ | | 1568.8 | 1569.1 |
| | | | +1 $C_6H_{13}OH$/−1 $H_2O$ | 1652.8 | 1653.0 |
| | | | +2 $C_6H_{13}OH$/−2 $H_2O$ | 1736.9 | 1736.9 |
| | | | +3 $C_6H_{13}OH$/−3 $H_2O$ | 1821.0 | 1820.6 |
| | | | +4 $C_6H_{13}OH$/−4 $H_2O$ | 1905.1 | 1904.7 |
| T9″ | 30.9 | $D_{96}-R_{107}$ | | 1321.6 | 1321.7 |
| T11[e] | 31.8 | $E_{128}-K_{144}$ | | 1927.8 | 1928.1 |
| T9 | 32.8 | $V_{92}-R_{107}$ | | 1810.9 | 1811.3 |
| T10 | 34.6 | $H_{108}-R_{127}$ | | 2404.0[c] | 2403.5 |
| T2 | 34.6 | $E_{15}-K_{31}$ | | 1846.9 | 1847.0 |
| $T4(SO)_2$[d] | 42.6/43.3 | $S_{39}-(MO)_2-R_{75}$ | | 4099.4[c] | |
| T4(SO)[d] | 45.9/46.1 | $S_{39}-(MO)-R_{75}$ | | 4083.4[c] | 4085 |
| T4 | 48.7/49.6 | $S_{39}-R_{75}$ | | 4067.4[c] | 4070 |

[a] The mass scale accuracy for the FAB experiment was 0.02% when calibration samples were rerun during the course of the peptide work. The mass accuracy of a given experiment will be affected by the ion statistics of the peptide of interest. There were no ambiguities relating to the mass assignments of the peptide ions, and all peptide ions were detected with an accuracy within 0.1% of the theoretical mass of the peptide of interest. [b] Calculated masses based on monoisotopic isotope distribution, except for T4 and T10 tryptic fragments, where isotopic masses are not resolved. [c] Average mass of $MH^+$ isotopic envelope. [d] These oxidative products were independently identified subsequent to the selective oxidative modification of the methionines in the parent peaks, which were then rechromatographed for identification purposes. [e] This peak contains an impurity with $[M+H]^+ = 1550$ and 1536. These masses are not native peptide tryptic fragments. The N-terminal tryptic fragment (T1) was not located; however T1−K would be 1536 and T1−Ac−Ala would be 1550.

to the generation of the methionine sulfoxide derivatives (Figure 2).

The mass spectrometric identification of the peptides associated with tryptic fragment T4 (which appears as a doublet; Figure 2) reveals the existence of a single resolved species with an average molecular mass of $m/z = 4070$, which is within the experimental error of the theoretically expected average mass for the T4 fragment (i.e., $m/e = 4067.4$ for $[M+H^+]$) (Table 1). Because the T4 fragment appears as an HPLC doublet and only one peptide mass was resolved, it is possible that the heterogeneity observed in the chromatogram is due to the deamidation of at least one Asn (see below), which would result in the conversion of the amide to the corresponding carboxylate with a corresponding change in $m/z$ of +1 amu. Since a heterogeneous mixture of peptides differing in mass by 1 amu would not be resolved under these experimental conditions, we cannot clearly identify the source of the heterogeneity in the chromatogram (Figure 2). However, the relatively narrow peak width observed in the mass spectrometer associated with the T4 chromatographic peak (i.e., 4−5 amu at full-width half-maximum) indicates that the major peptides corresponding to the doublet observed in the chromatogram do not differ in molecular weight by more then 1 amu. The existence of two distinct species that differ by 1 amu from the theoretical mass of the protonated T4 ion (i.e., $[M+H]^+$) can be rationalized by the possibility of deamidation at one of four potential deamidation sites in CaM, i.e., $Asn_{43}$, $Asn_{54}$, $Asn_{61}$, or $Asn_{71}$. Model hexapeptides have shown that the deamidation of the sequence Gly-Asn-Gly, present within the sequence of the wheat germ CaM T4 tryptic fragment as $Gly_{60}$-$Asn_{61}$-$Gly_{62}$, is particularly favored with a first-order rate constant at pH 8 of the order $10^{-1}$ $h^{-1}$ (Patel & Borchardt, 1990; Takemoto & Emmons, 1991; Oliyai et al., 1992). Furthermore, isoaspartate formation has been shown to occur at this site in CaM during in vitro storage (Potter et al., 1993). Thus, under our conditions of tryptic digestion (i.e., 8−10 h at pH 8), we expect considerable deamidation of $Asn_{61}$ and, in part, also of the other Asn residues, that are probably responsible for the observed heterogeneity in the HPLC chromatogram associated with tryptic fragment T4.

*Separation of Overlapping Peptides.* Two peptide fragments generated subsequent to tryptic digestion are not individually resolved in our chromatogram (i.e., a mixture of T2 and T10; Figure 2). Although the peak areas associated with these fragments do not appear to appreciably change upon exposure of CaM to $H_2O_2$, T10 contains two methionines and should be sensitive to modification by $H_2O_2$. Therefore, in order to resolve T2 from T10 we have taken advantage of the single cysteine located in T2, which upon modification with pyrenylmaleimide has a reduced retention time. In this manner, it has been possible to selectively resolve T10 (data not shown), which under these conditions was found to undergo significant levels of oxidative modification (Figure 3).

*Resolution of Central Methionine Subsequent to Proteolytic Digestion Using Endo GluC Protease.* While the majority of the peptides generated subsequent to tryptic cleavage were identified, it was not possible to separate and detect the tryptic fragments T1 ($Ala_1$-$Lys_{14}$) or T5−T6 (i.e., $Lys_{76}$-$Met_{77}$-$Lys_{78}$) by reversed-phase chromatography. While the former peptide contains no methionines, and is not likely to be oxidatively modified under these conditions (Vogt, 1995), the central methionine (i.e., $Met_{77}$) is part of a flexible hinge that comprises amino acids 75−83 in wheat germ CaM, and the analogous residues in animal CaM have been previously suggested to play a critical role with respect to modulation of the dynamics of the central helix by facilitating the association of CaM with target sequences of CaM-regulated proteins [reviewed by Crivici and Ikura (1995)]. We have therefore used Endo GluC protease to generate a complementary proteolytic map in order to assess the sensitivity of $Met_{77}$ to oxidative modification. Subsequent to the digestion of CaM with Endo GluC protease (see

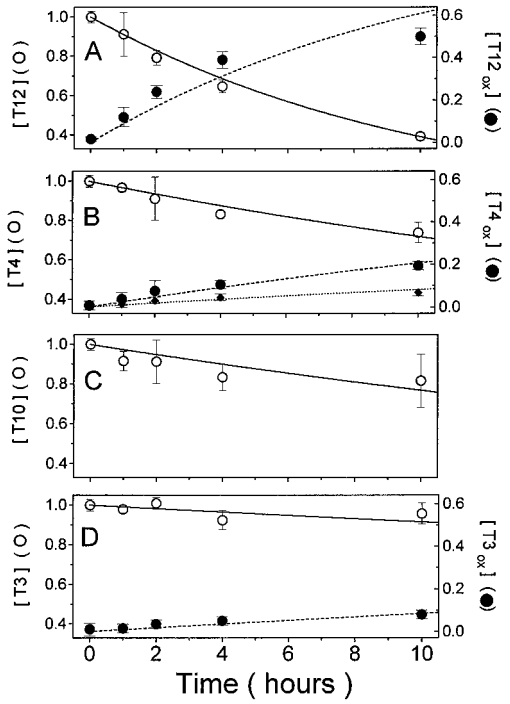


FIGURE 3: Differential sensitivity of tryptic fragments within calmodulin to oxidative modification by $H_2O_2$. Time course of oxidative modification of oxidatively sensitive parent tryptic fragments by $H_2O_2$ (○) and the associated appearance of the analogous peptides containing either one (●) or two (◆) sulfoxide products. Peptide concentrations were measured relative to the peak height of the unoxidized control sample. Experimental points represent means of two separate experiments, and correspond to tryptic fragments associated with T12 (A), T4 (B), T10 (C), and T3 (D) or their corresponding monosulfoxide oxidation products. We have also identified an oxidation product of T4 that contains two methionine sulfoxides (◆). In the case of T10, no oxidation products were resolved in these chromatograms. Error bars represent the standard deviation for two separate experiments. In all cases except for the T10 data, the parent tryptic fragment and associated oxidation product were simultaneously fit to a second-order rate equation (Levine, 1978), and the lines represent the best fit to the data. The associated rate constants are summarized in Table 2.

Experimental Procedures), we resolve 30 peptide fragments with retention times ranging between 3.7 and 54.5 min. There are 32 potential cleavage sites in CaM for Endo GluC protease that generate peptides with 2 or more amino acids, suggesting that our chromatographic conditions adequately separate the majority of the proteolytic fragments generated by the exhaustive digestion of CaM with Endo GluC. Reversed-phase HPLC and FAB mass spectrometric analysis of the peptide mixture obtained after Endo GluC proteolysis of native CaM revealed a peak with a retention time of 43 min which contained a peptide fragment with $[M+H]^+ = 1367$, corresponding to a single proteolytic fragment extending from $Phe_{69}$ to $Asp_{79}$ with a calculated monoistopic mass of $[M+H]^+ = 1365.7$ amu. This proteolytic fragment contains $Met_{73}$ and $Met_{77}$. The corresponding peak area in the chromatogram was virtually insensitive to oxidation of CaM with 5.0 mM $H_2O_2$ for 10 h. Moreover, FAB mass spectrometric analysis of the peak obtained from both native and oxidized CaM did not show any significant loss of the 1367 mass, indicating that this peptide fragment is not significantly modified by $H_2O_2$.

*Relative Sensitivities of Tryptic Fragments to Oxidative Modification.* Quantitation of the time course of the relative abundance of tryptic fragments corresponding to native CaM (Figure 3A) as well as the appearance of peaks associated with the oxidation products (Figure 3B) permits us to localize the oxidative damage associated with $H_2O_2$. It is apparent that the tryptic fragment T12 ($Val_{145}$−$Lys_{149}$) is most extensively oxidized, followed by tryptic fragments T4, T10, and T3. None of the peak heights or areas associated with the other tryptic peptide fragments are significantly affected. The respective oxidation products, T12 monosulfoxide (T12ox), T4 mono- and disulfoxide (T4ox and $T4ox_2$), and T3 sulfoxide, are apparent in the chromatogram (Figure 2), and their FAB mass spectrometric assignments are listed in Table 1. The oxidation products associated with T10 were not resolved in the chromatograms. Using the time course relating to the oxidative modification of T12, T4, T10, and T3 as well as the associated appearance of T12ox, T4ox, and T3ox, we were able to determine the second-order rate constants associated with the oxidative modification of these individual tryptic fragments. Ten hours of exposure to $H_2O_2$ results in the net oxidation of all 4 peptides, corresponding to an average of $1.3 \pm 0.1$ methionines per CaM. Of the oxidatively sensitive peptides, T12 (which contains $Met_{146}$ and $Met_{147}$ near the carboxyl terminus of CaM) is especially prone to oxidation, and accounts for greater than 45% of the oxidized peptides. The sensitivity of the vicinal methionines to ROS is particularly noteworthy, and is consistent with an enhanced chemical sensitivity of neighboring thioether functional groups to oxidation (Glass, 1990; Sanaullah et al., 1994), as well as with the enhanced reactivity of CaM at these sites with a number of nonphysiological oxidants (Walsh & Stevens, 1977; O'Neil et al., 1989).

*Solvent Accessibility of Methionine Residues and Relationship to Oxidative Modification.* The oxidative modification of individual methionine residues within CaM is expected to be related to both the oxidative potential of the individual amino acids and their relative exposure to $H_2O_2$. In order to access the relationship between the rate of oxidative modification at defined positions within CaM and the exposure of the methionines to $H_2O_2$, we have calculated the surface accessibility of the reactive sulfur atoms within the individual methionines in CaM, as described in Table 3. While the differences in the homologous crystal structures of the two recombinant forms of CaM from paramecium (Rao et al., 1993) and human (Chattopadhaya et al., 1992) used to model the structure of wheat germ CaM result in some uncertainty with respect to the exposure of individual methionines to solvent (see, for example, $Met_{77}$), it is apparent that the C-terminal vicinal methionines ($Met_{146}$ and $Met_{147}$) represent the two most exposed methionines within CaM. A quantitative comparison of the relationship between the oxidative modification of the methionines contained in tryptic fragments T12, T4, T10, and T3 with the calculated surface accessibility of the methionines contained within these tryptic fragments reveals a close correspondence subsequent to the normalization of both the rate of oxidative modification and the solvent accessibility of sulfur relative to the dipeptide Gly-Met (Table 2, Figure 4). The dipeptide Gly-Met was chosen for comparison purposes since it is not expected to exhibit either neighboring group effects that might modify the oxidation potential of methionine or significant steric effects that would modify the exposure of methionine to solvent (the sulfur in Gly-Met has a calculated surface accessibility that corresponds to 88% of what is calculated for a free sulfur atom; see Experimental Proce-

Table 2: Rate Constants Associated with Oxidative Modification of CaM Tryptic Fragments by Hydrogen Peroxide and Relationship to Surface Accessibility

| species | $k_{oxidation} \times 10^3$ ($M^{-1}$ $s^{-1}$)[a] | $k_{CaM}/k_{Gly\text{-}Met}$ | SA[b] (Å$^2$) | $SA/SA_{Gly\text{-}Met}$ | $(k_{CaM}/k_{Gly\text{-}Met})/(SA/SA_{Gly\text{-}Met})$ |
|---|---|---|---|---|---|
| Gly-Met | $8.1 \pm 1.0$ | 1.0 | 44.1 | 1.00 | 1.00 |
| $V_{145}-K_{149}$ (T12) | $5.3 \pm 0.4$ | $0.65 \pm 0.09$ | $49.3 \pm 0.1$ | $1.12 \pm 0.01$ | $0.58 \pm 0.08$ |
| $S_{39}-R_{75}$ (T4) | $1.9 \pm 0.1$ | $0.24 \pm 0.03$ | $23.4 \pm 4.2$ | $0.53 \pm 0.09$ | $0.45 \pm 0.10$ |
| $H_{108}-R_{127}$ (T10) | $1.5 \pm 0.3$ | $0.18 \pm 0.04$ | $11.1 \pm 2.2$ | $0.25 \pm 0.05$ | $0.72 \pm 0.21$ |
| $E_{32}-R_{38}$ (T3) | $0.50 \pm 0.05$ | $0.06 \pm 0.01$ | $7.9 \pm 1.1$ | $0.18 \pm 0.03$ | $0.33 \pm 0.08$ |

[a] Data were fit to a second-order rate equation (Levine, 1978), where the errors represent 67% confidence intervals as judged by the $\chi^2$ surface, using the *F*-statistic to estimate the limits of the errors. Fits were obtained from simultaneous fits of both the loss of parent tryptic fragments and the resulting generation of products, except for T10 where no oxidation products were identified. The *F*-statistic was obtained from standard statistical tables (Rohlf & Sokal, 1995). Errors were propagated assuming no cross-correlation (Bevington, 1969). [b] The surface accessibility (SA) of the methionines contained within each tryptic fragment was calculated as described under Experimental Procedures.

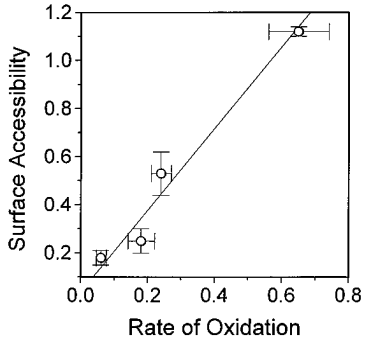


FIGURE 4: Relationship between calculated surface accessibility of methionines and rate of oxidative modification by $H_2O_2$. The surface accessibility to water of the sulfur atom for all eight methionines in wheat germ CaM was calculated as described under Experimental Procedures, and the total surface area of the sulfur atoms in each tryptic fragment was normalized relative to the exposed surface area of the sulfur in the peptide Gly-Met. Likewise, the rate of oxidative modification of the four sensitive tryptic fragments was normalized relative to the rate of oxidative modification of the exposed methionine in the dipeptide Gly-Met (Table 2). Error bars represent the standard deviation relating to the measurement of the rate of oxidative modification for the abscissa, and represent the calculated variability between the homologous structures for wheat germ CaM based on the two computed structures as described in Table 3. The line represents the relationship between surface accessibility and the rate of oxidative modification obtained from a linear regression [$F(x) = mx + B$] in which the sum of the squared deviations between the experimental fit and the data is minimized such that $m = 1.6 \pm 0.2$, $b = 0.06 \pm 0.08$, and the correlation coefficient is $0.984 \pm 0.009$.

Table 3: Calculated Surface Accessibilities of Methionines Obtained from Homology Mapping to Crystal Structure[a]

| | CaM source | | | | |
|---|---|---|---|---|---|
| | paramecium[b] | | human[c] | | |
| position | SA (Å$^2$) | percentage | SA (Å$^2$) | percentage | average (%) |
| $Met_{37}$ | 8.6 | 8.9 | 7.1 | 6.2 | $8 \pm 2$ |
| $Met_{52}$ | 16.0 | 16.5 | 12.2 | 10.7 | $14 \pm 4$ |
| $Met_{73}$ | 10.3 | 10.6 | 8.2 | 7.2 | $9 \pm 2$ |
| $Met_{77}$ | 0.14 | 0.1 | 27.9 | 24.4 | $12 \pm 17$ |
| $Met_{110}$ | 5.8 | 6.0 | 0.6 | 0.5 | $3 \pm 4$ |
| $Met_{125}$ | 6.8 | 7.0 | 9.0 | 7.9 | $8 \pm 1$ |
| $Met_{146}$ | 15.5 | 16.0 | 27.9 | 24.4 | $20 \pm 6$ |
| $Met_{147}$ | 33.9 | 34.9 | 21.3 | 18.7 | $27 \pm 11$ |
| total | 97.0 | 100.0 | 114.2 | 100 | 100 |

[a] The surface accessibility (SA) of sulfur atoms within individual methionines in CaM was calculated based upon the ability of water (radius is 1.6 Å) to come into contact with sulfur for two different structures of CaM as described under Experimental Procedures. There is a 85% and 90% sequence identity between paramecium and vertebrate CaM with wheat germ CaM. The coordinates for the structures of CaM were obtained from the Brookhaven data base for both paramecium (Rao et al., 1993; 1OSA) and human (Chattopadhyaya et al., 1992; 1CLL) recombinant forms of CaM expressed in *E. coli*. Posttranslational modifications involving the trimethylation of $Lys_{116}$ and the acetylation of the amino-terminal residue ($Ala_1$) as well as homologous amino acid substitutions were carried out prior to the energy minimization of the structure.

dures). This indicates that the relative rate of oxidative modification of the methionines within CaM is directly related to their relative exposure to $H_2O_2$ in the solvent. This suggests that the actual distribution of oxidized species can be calculated as described in Table 3 for all eight methionines contained within wheat germ CaM.

While there is a correlation between the calculated surface accessibility of methionines within CaM and the rate of oxidative modification by $H_2O_2$, the actual rate of oxidative modification is $62 \pm 6\%$ of the expected rate of oxidative modification based upon a comparison of the methionines contained within the four oxidatively sensitive tryptic fragments to the calculated solvent accessibility of the associated methionines obtained from the crystal structure of CaM, as discussed above. Since the conditions associated with oxidative modification were conducted at the same pH used in the crystallization of CaM, the reduced solvent accessibility of the methionines in CaM is consistent with previous results that indicate that there are substantial structural differences between the globular domains and the central helix in the crystal structure relative to that observed in solution [Trewhella et al., 1989; Wang, 1989; Barbato et al., 1992; Török et al., 1992; reviewed by Kretsinger (1992a,b)]. Alternatively, the uniform decrease in the rate of oxidative modification of the methionines in CaM by $H_2O_2$ relative to methionine in the dipeptide Gly-Met may be related to differences in the physical properties of CaM (e.g., high charge density) that functions to modify the rate of reaction with $H_2O_2$.

*Oxidative Modification of CaM by $H_2O_2$ at pH 7.5.* In general, we have emphasized experimental conditions relating to the oxidative modification of CaM that selectively oxidize methionine (i.e., pH 5.0; Vogt, 1995). However, it is clear that the solution structure of CaM at physiological pH is substantially different relative to pH 5.0 (Wang, 1989; Yao et al., 1994), suggesting that the sensitivity of the C-terminal vicinal methionines to oxidative modification by $H_2O_2$ might be altered. We have therefore assessed the relative sensitivities of the four major tryptic fragments to $H_2O_2$ at pH 7.5. Under these conditions (0.1 M KCl, 1 mM $MgCl_2$, 0.1 mM $CaCl_2$, and 50 mM HEPES at pH 7.5), we find that in addition to the oxidative modification of T12, T4, T10, and T3, the tryptic fragments T2 (which contains $Cys_{27}$) and T11 (which contains $Tyr_{139}$) are also modified, consistent with the expected sensitivity of cysteine and

tyrosine to oxidative modification at neutral pH. However, the four methionine-rich tryptic fragments (T12, T4, T10, and T3) remain the major sites of oxidative modification, and their relative sensitivities to oxidative modification are virtually identical to that observed at pH 5.0 (data not shown), indicating that pH-dependent modifications within the tertiary structure of CaM do not substantially alter the relative susceptibility of the methionines in CaM to oxidative modification.

*Relationships between Oxidative Modifications and the Ability of CaM To Activate the PM-Ca-ATPase.* In order to assess the functional significance of the oxidative modification of CaM, we assayed the ability of CaM to activate the PM-Ca-ATPase (which, like other target proteins that are directly regulated by CaM, contains an autoregulatory sequence that functions to modulate the rate of calcium transport across the plasma membrane). One observes that native (unoxidized) wheat germ CaM is able to activate the PM-Ca-ATPase by more than 2-fold relative to the control (no added CaM; Figure 5A), consistent with earlier observations regarding the ability of CaM isolated from plant and vertebrate animal sources to activate the PM-Ca-ATPase to a similar extent (Strasburg et al., 1988; Yao et al., 1994). Upon limited oxidation of Met to MetSO (such that on average 1.3 ± 0.1 Met is oxidized per CaM), CaM is no longer able to fully activate the PM-Ca-ATPase (i.e., there is a 60−70% decrease in $V_{max}$ relative to the unactivated control; Figure 5B). The extent of inhibition closely parallels the amount of T12 peptide that becomes oxidatively modified (60% of T12 becomes oxidatively modified; Figure 3), suggesting that the oxidative modification of these sites may play a role in the loss of CaM's ability to activate the ATPase. There is a corresponding 5-fold increase in the amount of CaM necessary to activate the PM-Ca-ATPase as a function of oxidative modification, as assessed by the amount of CaM necessary for half-maximal activation (Figure 5C). This is consistent with the established role of methionine in forming the binding cleft for target protein activation (Crivici & Ikura, 1995).

No additional activation of the PM-Ca-ATPase is observed upon increasing the concentration of wheat germ CaM from 0.2 $\mu$M to 3 $\mu$M (Figure 5A). Since the oxidatively modified CaM always contains a mixed population of species, including native CaM, the decrease in $V_{max}$ associated with increasing degrees of oxidative modification (irrespective of the amount of CaM added) indicates that the oxidatively modified CaM can still bind to the autoinhibitory domain of the erythrocyte PM-Ca-ATPase. This indicates that the oxidative modification of CaM results in a functionally incompetent protein that upon binding to the autoinhibitory domain of the PM-Ca-ATPase is no longer able to activate the PM-Ca-ATPase. The close correlation between the amount of oxidative modification to T12 and the decrease in $V_{max}$ indicates that oxidatively modified CaM competes with unmodified (native) CaM from productively associating with the autoinhibitory domain of the PM-Ca-ATPase. A quantitative description relating to the CaM-dependent activation of the PM-Ca-ATPase is provided in the legend to Figure 5, where we find that the inhibition of the PM-Ca-ATPase subsequent to the oxidative modification of CaM can be described if one assumes that some of the species of oxidatively modified CaM function as a simple noncompetitive antagonist of the PM-Ca-ATPase.

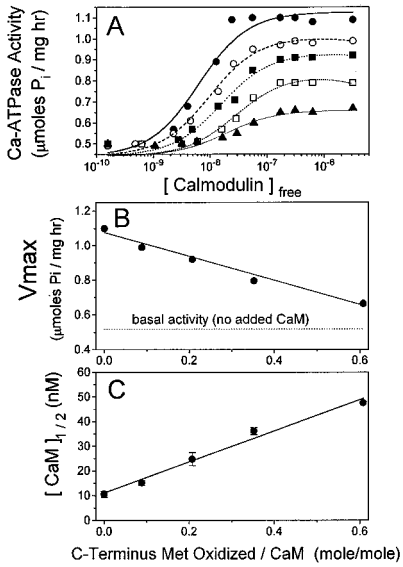


FIGURE 5: Calmodulin-dependence of activation of plasma membrane Ca-ATPase. The ATPase activity of the PM-Ca-ATPase from porcine erythrocyte ghosts was measured in the presence of native CaM (●), and subsequent to the oxidation of CaM for 1 h (○), 2 h (■), 4 h (□), and 10 h (▲) (A). Data for native CaM were fit using eq 5 as described under Experimental Procedures, where in this case $Y$ represents the normalized CaM-dependent activation of the PM-Ca-ATPase, $K_1$ represents the association constant for CaM binding to and activating the PM-Ca-ATPase, and $[X]_{free}$ represents the free molar concentration of CaM in solution as determined from eq 1. In the case of oxidatively modified CaM, the relationship between ATPase activity and $[CaM]_{free}$ was fit using eq 11, which assumes that some of the species of oxidatively modified CaM function as simple noncompetitive antagonists of the PM-Ca-ATPase. The recovered parameters indicate that $K_a = (1 \pm 1) \times 10^8$ M$^{-1}$ and $K_I = (2.5 \pm 0.7) \times 10^4$ M$^{-1}$, respectively. This corresponds to a free energy of activation of $-11.2 \pm 0.2$ kcal mol$^{-1}$ K$^{-1}$ and $-6.0 \pm 0.2$ kcal mol$^{-1}$ K$^{-1}$ for the native and oxidatively modified CaM, respectively. The maximal velocity (**$V_{max}$**; panel B**)** and the concentration of CaM necessary for half-activation of the ATPase (**$[CaM]_{1/2}$**; panel C) as a function of the number of carboxyl-terminal methionines oxidized to their corresponding sulfoxides are illustrated. The data were fit assuming a two-state model (eq 10) in which both $V_{max}$ and $[CaM]_{1/2}$ are a linear combination of the associated parameters that describe $CaM_{native}$ and $CaM_{oxidized}$, as described above. The associated amplitudes corresponding to the native and structurally modified populations of CaM were found to correspond closely with the extent of oxidative modification associated with the carboxyl-terminal vicinal methionines. Therefore, the line drawn through the data points in panels B and C assumes the amplitudes relating to the oxidative modification of the C-terminal vicinal methionines (Figure 3A; Table 2), and the associated $V_{max}$ and $[CaM]_{1/2}$ for native and the modified CaM species were allowed to vary. Native and oxidatively modified CaM were found to have associated maximal velocities of 1.08 and 0.38 $\mu$mol of $P_i$ mg$^{-1}$ h$^{-1}$, respectively. The $[CaM]_{1/2}$ for native and oxidatively modified CaM was found to be 11 and 74 nM, respectively. There was no close correlation between alterations in $V_{max}$ and $[CaM]_{1/2}$ and the oxidative modification of methionines at other sites within CaM. Ca-ATPase activity was measured at 25 °C in a reaction mixture containing 0.4 mg/mL protein (approximately 15 nM Ca-ATPase), 0.1 M KCl, 5 mM $MgCl_2$, 100 $\mu$M EGTA, 50 mM MOPS (pH 7.0), and 3 $\mu$M A23187, and phosphate release was measured as described previously (Lanzetta et al., 1979). In all cases, the free calcium concentrations were 30 $\mu$M, which fully saturates the calcium binding sites of the erythrocyte Ca-ATPase, permitting a measurement of maximal velocities in the presence of increasing concentrations of CaM. A23187 functions as a calcium ionophore to prevent back-inhibition of the ATPase by accumulated calcium inside the ghosts. Measured ATPase activities represent the mean of two separate measurements, and had a standard deviation of 5%.

*Alterations in Calcium Concentrations Necessary To Activate the PM-Ca-ATPase.* The physiological role of the PM-Ca-ATPase is to maintain low resting calcium levels at a level below 0.1 $\mu$M in normal healthy cells [reviewed by Carafoli (1987)]. Any decreases in the calcium sensitivity of oxidatively modified CaM to activate the PM-Ca-ATPase will therefore have a detrimental effect upon cellular metabolism and signaling, and a more physiological estimation of the effects of oxidative modification of CaM upon cellular metabolism involves the consideration of the influence of oxidative damage to CaM at physiological calcium concentrations. While modulation of the available free CaM to activate the ATPase may represent an additional level of cellular regulation [Blackshear et al., 1992; reviewed by Blackshear (1993)], for simplicity we have considered the influence of oxidative modification to CaM in the presence of saturating CaM (Figure 6A). One observes an analogous decrease in the maximal calcium-dependent ATPase activity ($V_{max}$; Figure 6A,B) as observed upon titration of the ATPase with CaM in the presence of saturating calcium concentrations (Figure 5A,B). Subsequent to oxidative modification of CaM by $H_2O_2$, there is a relatively modest (less than 2-fold) increase in the amount of calcium necessary to activate the ATPase (Figure 6C). However, since CaM binding to the PM-Ca-ATPase does not modify the apparent affinities of the calcium binding sites on the PM-Ca-ATPase (see legend to Figure 6), the similar calcium concentrations for native and oxidatively modified CaM with respect to the half-maximal level of calcium necessary for the CaM-dependent activation of the PM-Ca-ATPase indicate only that oxidatively modified CaM is able to compete with native CaM for the binding site on the ATPase at normal physiological levels of calcium.

*Measurement of Calcium Binding Stoichiometry.* A quantitative assessment relating to the influence of oxidative modifications to CaM requires that possible alterations with respect to the ability of CaM to bind calcium be considered. We have therefore used radioactive calcium to directly measure the total number of calcium binding sites in native and oxidatively modified CaM. The latter sample was exposed to $H_2O_2$ for 10 h at pH 5.0, and was subsequently separated from unreacted $H_2O_2$, lyophilized, and equilibrated with buffer as described under Experimental Procedures. We find that native CaM binds 4.07 $\pm$ 0.05 mol of calcium per mole of CaM, in agreement with the presence of four known calcium binding sites in CaM (Babu et al., 1985). Subsequent to the oxidative modification of 1.3 $\pm$ 0.1 mol of methionine per CaM, we find that the oxidatively modified CaM binds 3.9 $\pm$ 0.2 mol of calcium per mole of CaM. This indicates that under saturating calcium concentrations there is no loss in the number of calcium binding sites for oxidatively modified CaM.

*Electrophoretic Mobility of Oxidatively Modified CaM.* Subsequent to the denaturation of CaM in the presence of SDS, the sensitivity of the relative mobility of CaM on polyacrylamide gels has proven to be very sensitive to alterations in the structural properties of CaM associated with calcium binding (Klee et al., 1979; Maune et al., 1992; Zhang et al., 1994). We observe that both native and oxidatively modified CaM undergo analogous mobility shifts associated with calcium binding on SDS−polyacrylamide electrophoretic gels ($MW_{apparent}$ = 15 300) relative to that seen when CaM is denatured in the presence of EGTA ($MW_{apparent}$ = 24 500; Figure 7A), and that the shift in the apparent molecular weight of CaM is in correspondence with previous results observed for native CaM (Burgess et al., 1980). The oxidatively modified CaM behaves as a single population,

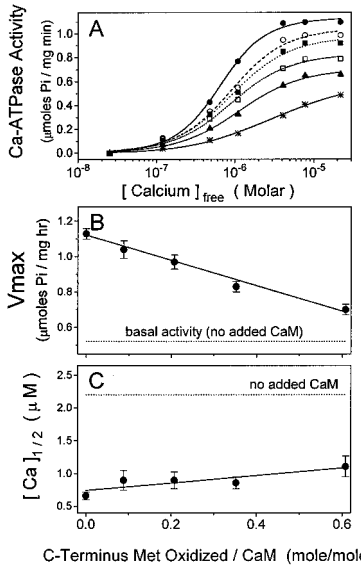


FIGURE 6: Calcium-dependence of calmodulin activation of plasma membrane Ca-ATPase. (A) The calcium-dependent ATPase activity of the PM-Ca-ATPase from porcine erythrocyte ghosts was measured in the presence of native CaM (●), and subsequent to the oxidation of CaM for 1 h (○), 2 h (■), 4 h (□), and 10 h (▲). Free calcium concentrations were determined as described under Experimental Procedures. The normalized calcium-dependent ATPase activity was obtained in the presence of 0.6 $\mu$M CaM, which is sufficient to fully saturate the CaM binding sites of the erythrocyte Ca-ATPase in all cases (see Figure 5). This permits an estimate of maximal velocities in the presence of increasing concentrations of calcium. The calcium-dependent ATPase activity of the PM-Ca-ATPase in the absence of the added CaM is shown for comparison (*). The calcium-dependent activation of the Ca-ATPase was fit using eq 6, assuming that the oxidatively modified CaM associated with the PM-Ca-ATPase did not contribute to the observed calmodulin-dependent ATPase activity. The free energies associated with calcium activation of the PM-Ca-ATPase in the presence of native CaM (●) corresponded to $\Delta G_1 = -8.2 \pm 1.5$ kcal mol$^{-1}$ K$^{-1}$ and $\Delta G_2 = -16.9 \pm 0.9$ kcal mol$^{-1}$ K$^{-1}$. The free energies associated with calcium activation of the PM-Ca-ATPase in the absence of CaM (*) corresponded to $\Delta G_1 = -8.2 \pm 0.1$ kcal mol$^{-1}$ K$^{-1}$ and $\Delta G_2 = -15.1 \pm 0.1$ kcal mol$^{-1}$ K$^{-1}$. The maximal velocity (B) and the concentration of calcium necessary for half-activation of the ATPase as a function of the number of methionines oxidized to their corresponding sulfoxides are illustrated. The data in panels B and C were fit assuming a two-state model in which both $V_{max}$ and $[calcium]_{1/2}$ are a linear combination of the associated parameters that decribe $CaM_{native}$ and $CaM_{oxidized}$, as described for the analogous panels in Figure 5. The associated amplitudes corresponding to the native and oxidatively modified populations of CaM were found to correspond closely with the extent of oxidative modification associated with the C-terminal vicinal methionines, and for reasons discussed in Figure 5 were held fixed in fitting the data shown in panels B and C. There was no apparent correlation with respect to the oxidative modification of methionines at other sites within CaM. Native and oxidatively modified CaMs were found to have associated maximal velocities of 1.12 and 0.41 $\mu$mol of $P_i$ mg$^{-1}$ h$^{-1}$, respectively. The $[calcium]_{1/2}$ for native and oxidatively modified CaM was found to be 0.7 and 1.3 $\mu$M, respectively. Experimental buffer contained 0.4 mg/mL protein (approximately 15 nM PM-Ca-ATPase), 0.1 M KCl, 5 mM $MgCl_2$, 100 $\mu$M EGTA, 50 mM MOPS (pH 7.0), and 3 $\mu$M A23187. A23187 functions as a calcium ionophore to prevent back-inhibition of the ATPase by accumulated calcium inside the erythrocyte ghosts. Temperature was 25 °C. Measured ATPase activities represent the mean of two separate measurements, and had a standard deviation of 5%.

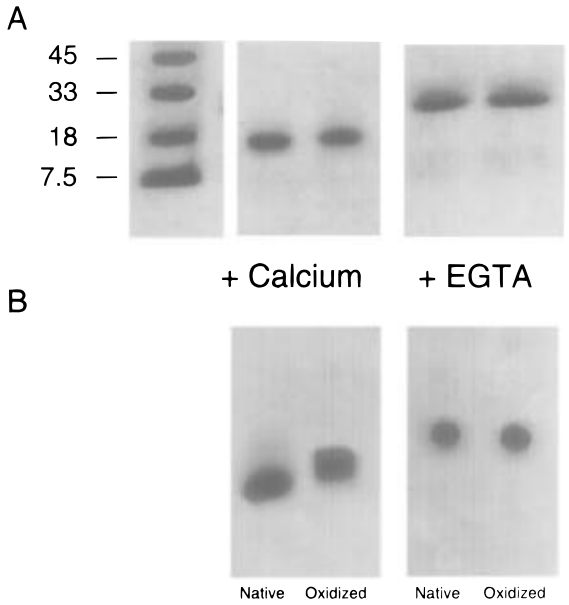


FIGURE 7: Electrophoretic mobility of native and oxidatively modified CaM on SDS−PAGE. (A) SDS−PAGE was performed as described by Laemmli (1970), where 10 $\mu$g of denatured CaM was applied to each lane on a 7−17% acrylamide gradient at pH 8.8. BioRad's kaleidoscope prestained molecular mass standards are shown in the left lane with the associated molecular mass, and represent aprotinin (7.5 kDa), lysozyme (18 kDa), soybean trypsin inhibitor (32.6 kDa), and carbonic anhydrase (45 kDa). (B) Native gels were performed as described by Trybus and Lowey (1985), where 6 $\mu$g of native CaM was applied to a 10% polyacrylamide gel at pH 8.5. Sample conditions included 1 mM $CaCl_2$ (+Ca) or 1 mM EGTA (+EGTA) in both sample and running buffers. Oxidized CaM refers to CaM subsequent to the oxidative modification of 1.3 ± 0.1 methionines per CaM using $H_2O_2$ as described under Experimental Procedures. Protein bands were visualized using Coomassie brilliant blue.

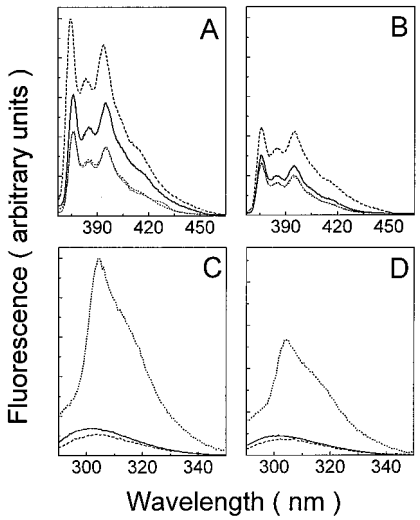


FIGURE 8: Fluorescence spectral changes associated with calcium activation and peptide binding. Fluorescence emission spectra associated with native (A, C) and oxidatively modified (B, D) CaM using either pyrenylmaleimide (at $Cys_{27}$; A, B; $\lambda_{ex}$ = 351 nm) or $Tyr_{139}$ (C, D; $\lambda_{ex}$ = 275 nm) to monitor structural changes associated with either the amino- or the carboxyl-terminal domains of CaM, respectively. Oxidative modification to CaM involves the oxidative modification of 1.3 ± 0.1 methionines per CaM using $H_2O_2$ as described under Experimental Procedures. Spectra were taken in the presence of either EGTA (dashed line), calcium (solid line), calcium + F52 peptide (dotted line), or calcium + C25W peptide (dot−dash line; panels A and B only). Spectra were taken at 25 °C of 24 $\mu$M CaM in 0.1 M HEPES (pH 7.5), 0.1 M KCl, and either 0.1 mM $CaCl_2$ or 0.1 mM EGTA. When appropriate, either F52 or C25W peptides were added in 2-fold molar excess. Emission spectra were taken at 0.5 nm intervals, using emission slits with a 4 nm bandwidth.

indicating that all species undergo analogous structural changes. There is no apparent heterogeneity or increase in the width of the band of the oxidatively modified CaM on the gel relative to native CaM, indicating that oxidative modification of a limited number of methionines does not dramatically alter the structure of CaM, or affect CaM's ability to undergo calcium-dependent structural changes.

Analogous results are observed after electrophoresis of native and oxidatively modified CaM using native gel conditions (Figure 7B), where the mobility of CaM is more sensitive to structural modifications involving CaM's tertiary structure (Maune et al., 1992). Under these conditions, one still observes calcium-dependent changes in the electrophoretic mobility of both native and oxidized CaM (Figure 7B), indicating that the tertiary structure of oxidatively modified CaM remains sensitive to calcium binding. However, while the electrophoretic mobilities of native and oxidatively modified CaM are similar in the absence of calcium, upon calcium binding one observes a significantly reduced electrophoretic mobility of oxidatively modified CaM. The altered hydrodynamic properties of oxidatively modified CaM observed using native gels suggest that the selective oxidation of one of the carboxyl-terminal vicinal methionines perturbs the tertiary structure of CaM.

*Calcium-Dependent Structural Changes Associated with Calcium Activation of CaM.* Alterations in the ability of CaM to undergo calcium-dependent structural changes were directly assessed using fluorescence spectroscopy to monitor alterations in the environment surrounding either a covalently attached fluorophore (i.e., pyrenylmaleimide) on $Cys_{27}$, located in calcium binding site I in the amino-terminal domain, or the intrinsic fluorophore ($Tyr_{139}$), located in calcium binding site IV in the carboxyl-terminal domain (Figure 1). There is a substantial decrease in the fluorescence intensity of pyrene associated with oxidative modification to CaM (Figure 8A,B), indicating that the oxidative modification of a limited number of methionines alters the environment around pyrene. However, both native and oxidatively modified CaM undergo analogous calcium-dependent alterations in their quantum yield, indicating that oxidatively modified CaM undergoes analogous structural changes in calcium binding loop I upon calcium binding. Likewise, analogous calcium-dependent increases in the fluorescence intensity of $Tyr_{139}$ are observed in both native and oxidatively modified CaM upon calcium binding, suggesting that while oxidative modification may perturb the tertiary structure of CaM, both the carboxyl- and amino-terminal domains of CaM undergo analogous calcium-dependent structural changes upon calcium binding.

In order to more quantitatively examine the calcium-dependent changes in fluorescence associated with pyrenylmaleimide (on $Cys_{27}$) and $Tyr_{139}$, we have measured the average fluorescence lifetimes of these chromophores using frequency-domain fluorescence spectroscopy, as described previously for native CaM (Yao et al., 1994). The average fluorescence lifetimes of pyrene and tyrosine are directly related to alterations in the structure of CaM (Royer, 1993). We have therefore used the average lifetime to monitor structural changes in CaM as a function of both calcium binding and oxidative modification. Subsequent to the

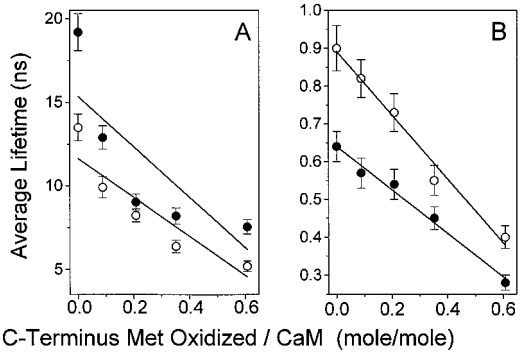


FIGURE 9: Oxidative modification decreases average fluorescence lifetimes. Average lifetime of (A) pyrenylmaleimide CaM and (B) $Tyr_{139}$ in the presence of either 0.1 mM $CaCl_2$ (○) or 0.2 mM EGTA (●). Fluorescence lifetimes were measured using frequency-domain fluorescence spectroscopy, as previously described (Yao et al., 1994) assuming phase errors of 0.2° and a modulation error of 0.005. Average lifetimes were calculated as described under Experimental Procedures. CaM was oxidatively modified using $H_2O_2$ for variable periods of time, as described under Experimental Procedures. The line represents a fit to a two-state model using eq 10, and assumes that the observed lifetime is a linear combination of the relative amplitudes of native CaM and a structurally modified CaM species that corresponds to the extent of modification to the C-terminal vicinal methionines in tryptic fragment 12. Using this model, the recovered average lifetime that corresponds to a population of CaM in which the carboxyl-terminal methionines are quantitatively modified corresponds to (A) 0.1 ns (○) and 0.3 ns (●) and (B) 0.1 ns (○) and 0.05 ns (●). Experimental conditions: 25 °C in 0.1 M HEPES (pH 7.5), 0.1 M KCl, and either 0.1 mM $CaCl_2$ or 0.1 mM EGTA. CaM concentration was 0.6 $\mu$M (A) or 24 $\mu$M (B).

oxidative modification of CaM, the fluorescence intensity and average lifetime associated with pyrenylmaleimide (Figures 8A and 9A) and tyrosine (Figures 8B and 9B) become smaller, irrespective of whether or not calcium is bound. The analogous decrease in the steady-state fluorescence intensity and excited state lifetime associated with both pyrene and tyrosine chromophores upon oxidative modification indicates that the observed fluorescence is representative of the entire population of CaM, and that oxidation does not result in any selective quenching of the fluorescence signals associated with the oxidatively modified population of CaM.

The large decrease in the fluorescence intensity and average lifetime of pyrenylmaleimide and tyrosine subsequent to oxidative modification indicates that the environment surrounding these chromophores becomes more polar (Lakowicz, 1983; Schöneich et al., 1995), suggesting that the oxidative modification of selected residues within CaM disrupts the tertiary structure of both the amino- and carboxyl-terminal domains of CaM to enhance the solvent accessibility of these fluorescent reporter groups. Oxidation experiments were carried out both before and after labeling CaM with pyrenylmaleimide, and under our experimental conditions (i.e., pH 5.0), neither the single cysteine present in the unlabeled CaM nor the pyrene covalently attached to $Cys_{27}$ is oxidatively modified as assessed by a titration of free cysteine using DTNB, through measurements of the steady-state and lifetime-resolved fluorescence associated with pyrene, and as a result of the lack of any modification in the relative intensity or retention time associated with tryptic fragment T2 (which contains $Cys_{27}$). The observed lack of reactivity of either cysteine or pyrene may in part be related to the minimal solvent accessibility of this $Cys_{27}$, which is buried within CaM's tertiary structure (Yao et al., 1994),

The calcium-dependent changes in the average lifetime and steady-state fluorescence intensity of PM-labeled ($Cys_{27}$) CaM and native ($Tyr_{139}$) CaM were used to assess the influence of the oxidative modifications on the structural changes associated with the calcium-dependent activation of the amino and carboxyl domains of CaM, respectively. One observes an analogous calcium-dependent change in both the steady-state fluorescence intensity and the average fluorescence lifetime irrespective of the extent of oxidative modification (Figures 8 and 9). The fact that native and oxidatively modified CaM undergo similar steady-state and lifetime-resolved fluorescence changes upon calcium binding indicates that the globular domains in oxidatively modified CaM undergo similar structural changes upon calcium binding to that observed in native CaM. This is consistent with the observed calcium-dependent shifts in electrophoretic mobility on polyacrylamide gels that also suggest that oxidatively modified CaM undergoes calcium-dependent structural changes in the presence of saturating calcium concentrations (Figure 7).

*Changes in Calcium Affinity Associated with Oxidative Modification of CaM.* In order to measure the calcium affinity of both native and oxidatively modified CaM, we assessed the structural changes associated with calcium activation of the amino and carboxyl domains of CaM using the respective fluorescence changes associated with PM-labeled ($Cys_{27}$) CaM (Figure 10A) and native ($Tyr_{139}$) CaM (Figure 10B). Free calcium concentrations were determined using the fluorescent calcium indicator FURA-2, and were based on initial estimates of free calcium concentrations calculated from a consideration of the multiple equilibrium between calcium and all added ligands as described under Experimental Procedures.

As described previously (Yao et al., 1994), we observe upon systematic variation of the free calcium concentration in native wheat germ CaM that the changes in the fluorescence intensity of $Tyr_{139}$ are biphasic (Figure 10B), consistent with previous measurements that indicate $Tyr_{139}$ (or its equivalent) to be sensitive to calcium binding to the amino-terminal domain of CaM from *Drosophila melanoganster* (Maune et al., 1992), scallop (Yazawa et al., 1990), and bovine (Wang et al., 1982) sources. In contrast, the fluorescence intensity of pyrene increases monophasically over the same broad range of calcium concentrations associated with activation of the erythrocyte Ca-ATPase, indicating that the structural changes sensed by these two chromophores are differentially sensitive to the calcium occupancy of individual calcium binding sites within CaM.

The direct correspondence between the calcium-dependent changes in the average lifetime and steady-state fluorescence of pyrene allows us to directly relate the fluorescence signal to the extent of calcium binding, as described in the legend to Figure 10. We find the pyrene is sensitive to the occupancy of the single class of calcium sites, and the structural changes assessed by pyrene undergo a free energy change of $-11.6 \pm 0.1$ kcal mol$^{-1}$ K$^{-1}$ upon calcium binding. Subsequent to the selective oxidation of CaM by $H_2O_2$, we observe a $2.0 \pm 0.1$ kcal mol$^{-1}$ K$^{-1}$ decrease in the affinity for calcium ions in the amino-terminal domain of CaM as monitored by pyrenylmaleimide (Table 4), corresponding to a 30-fold reduction in calcium affinity.

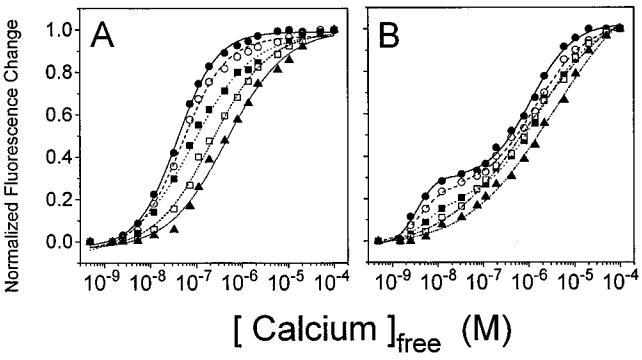


FIGURE 10: Calcium-dependent structural changes associated with activation of CaM. Normalized fluorescence intensity changes, $[|-(F - F_0)/(F_{max} - F_0)|]$, are illustrated as a function of free calcium concentration, where $F$ is the observed fluorescence relative to the initial fluorescence ($F_0$) and maximum fluorescence ($F_{max}$) of either (A) pyrenylmaleimide covalently linked to $Cys_{27}$, where $F_{max}$ corresponds to a 47 ± 3% decrease relative to $F_0$, or (B) the single $Tyr_{139}$, where $F_{max}$ corresponds to a 13 ± 2% increase relative to $F_0$. Samples include native CaM (●), and subsequent to the oxidative modification of 0.33 Met (○), 0.59 Met (■), 0.92 Met (□), and 1.3 methionines (▲) per CaM to the corresponding sulfoxide. The strategy used to fit these data involved the selection of the simplest model that could adequately describe the data involving the calcium-dependent activation of the PM-Ca-ATPase by native CaM (●), as judged both by the random residuals and by the lack of improvement in the variance upon the use of additional fitting parameters. As a result, different models were used to describe the calcium-dependent changes in the fluorescence associated with pyrenylmaleimide (A) and tyrosine (B). In the case of pyrenylmaleimide, eq 5 adequately described the data for native CaM (A), where $\Delta G_{native} = -10.0 \pm 0.1$ kcal $M^{-1}$ $K^{-1}$. Using this value to describe the association constant for native CaM, the data set in panel A was fit simultaneously using eq 10. The associated fits are shown in panel A, where $\Delta G_{oxidized} = -8.0 \pm 0.1$ kcal $M^{-1}$ $K^{-1}$. The associated amplitudes ($1 - \alpha_i$ in eq 10) for the oxidatively modified population of CaM subsequent to 1 (○), 2 (■), 4 (□), and 10 (▲) hours of incubation with $H_2O_2$ (see Experimental Procedures) were 0.13, 0.32, 0.54, and 0.76, in close agreement with the observed extent of oxidative modification to the C-terminal vicinal methionines in T12 (Figure 3). The bimodal dependence of tyrosine fluorescence associated with calcium activation shown for native CaM in panel B was fit using the equation given in footnote *a* of Table 4. For native CaM, the free energies associated with calcium activation are $\Delta G_a = -8.4$ kcal $mol^{-1}$ $deg^{-1}$, $\Delta G_b = -16.1$ kcal $mol^{-1}$ $deg^{-1}$, $\Delta G_1 = -11.6$ kcal $mol^{-1}$ $deg^{-1}$, and $b = 0.61$. Using these values to describe the binding isotherm for native CaM, the data set in panel B was fit simultaneously using eq 10. The resultant fits are shown in panel B. The free energy changes associated with the calcium activation of oxidatively modified CaM species are $\Delta G_a = -6.9$ kcal $mol^{-1}$ $deg^{-1}$, $\Delta G_b = -13.8$ kcal $mol^{-1}$ $deg^{-1}$, and $\Delta G_1 = -9.5$ kcal $mol^{-1}$ $deg^{-1}$. The associated amplitudes ($1 - \alpha_i$ in eq 10) for the oxidatively modified population of CaM subsequent to 1 (○), 2 (■), 4 (□), and 10 (▲) h of incubation with $H_2O_2$ (see Experimental Procedures) were 0.18, 0.39, 0.41, and 0.69, in close agreement with the observed extent of oxidative modification to the C-terminal vicinal methionines in T12 (Figure 3). Sample conditions include 0.1 M KCl, 1 mM $MgCl_2$, 0.1 M HEPES (pH 7.5), and either 0.6 $\mu$M CaM (A) or 23.8 $\mu$M CaM (B). Calcium was added to yield the desired free concentration, as described under Experimental Procedures.

A quantitative interpretation of the observed calcium-dependent change in the tyrosine signal is complicated by the presence of calcium-dependent changes in the static quenching of tyrosine (Yao et al, 1994). If one assumes that there is a linear dependence between the fluorescence signal and calcium binding, one can recover the binding energies associated with calcium activation of native and oxidatively modified CaM, as described in the legend to Figure 10. The change in the fluorescence signal associated with $Tyr_{139}$ can be adequately described by a model involving structural coupling between tyrosine's local environment and the occupancy of two classes of calcium binding sites (Figure 10B), and is consistent with earlier measurements indicating (i) that CaM must adopt intermediate conformations corresponding to partial occupancy of the four calcium binding sites and (ii) that there is a conformational coupling between the opposing globular domains in CaM upon calcium binding (Klee, 1977; Seamon, 1980; Johnson, 1983; Yoshida et al., 1983; Thulin et al., 1984; Wang et al., 1984; Babu et al., 1988; Maune et al., 1992; MacKall & Klee, 1991; Török et al., 1992; Kilhoffer et al., 1992; Yao et al., 1994; Pedigo & Shea, 1995). One observes that the free energies of activation associated with the tyrosine signal are in good agreement with other direct structural measurements in which the free energies associated with calcium activation were measured (Pedigo & Shea, 1995), and that subsequent to oxidative modification there is an average reduction in the free energies of activation associated with calcium activation at $Tyr_{139}$ of about 2.3 ± 0.2 kcal $mol^{-1}$ $K^{-1}$ (Table 4). The similar alteration in binding energies associated with calcium activation reported by pyrene (at $Cys_{27}$) and $Tyr_{139}$ indicates that the oxidative modification of CaM modifies the calcium-dependent structural changes associated with calcium activation at these spatially distant sites in a similar manner. This implies that the oxidative modification of a limited number of methionines alters the global structural properties of CaM.

*Peptide Binding to CaM.* The inability of the oxidatively modified CaM to activate the PM-Ca-ATPase could arise as a result of its inability to bind to the target sequence in the ATPase, or, alternatively, that binding of CaM occurs in a nonproductive manner as suggested by the ability of oxidatively modified CaM to act as a noncompetitive inhibitor of native CaM (Figure 5). In order to directly assess the binding affinity of CaM to target sequences, we have used the fluorescence changes associated with peptide binding of (i) pyrenylmaleimide (PM) at $Cys_{27}$ and (ii) $Tyr_{139}$ to measure the binding affinity between the amino and carboxyl domains of CaM and two target peptides that represent (i) the autoregulatory domains associated with the PM-Ca-ATPase (C25W) and (ii) a homolog to the MARCKS protein (F52)(Crivici & Ikura, 1995). The latter peptide has the advantage that it contains no tryptophans or tyrosines that would interfere with the detection of CaM's tyrosine fluorescence (CaM also contains no tryptophans).

We observe that in native CaM there is a 29 ± 2% and a 34 ± 3% decrease in the fluorescence intensity of PM at $Cys_{27}$ upon binding either F52 (Figures 8A and 11A) or C25W peptides (Figure 8A). The decrease in fluorescence intensity suggests that the structural rearrangements associated with peptide binding to CaM enhance the solvent exposure (and polarity) of PM (Yao et al., 1994). There is a corresponding 6.6-fold increase in the fluorescence intensity of $Tyr_{139}$ in native CaM upon association with F52 (Figures 8B and 11B). Subsequent to the limited oxidative modification of CaM in which one of the carboxyl-terminal methionines (either $Met_{146}$ or $Met_{147}$) is preferentially oxidized to the corresponding sulfoxide (Figure 2; Table 1), there is a large decrease in the maximum fluorescence change upon peptide binding associated with both pyrenylmaleimide (Figures 8A and 11A) and tyrosine (Figures 8B and 11B). The decrease in pyrene fluorescence associated with peptide

Table 4: Free Energy Changes Associated with Calcium Activation of Calmodulin[a]

| reporter group | native CaM (kcal mol$^{-1}$ K$^{-1}$) | | | oxidized CaM (kcal mol K) | | | difference, $\Delta\Delta G = \Delta G_{oxidized} - \Delta G_{native}$ (kcal mol$^{-1}$ K$^{-1}$) | | |
|---|---|---|---|---|---|---|---|---|---|
| | $\Delta G_a$ | $\Delta G_b$ | $\Delta G_1$ | $\Delta G_a$ | $\Delta G_b$ | $\Delta G_1$ | $\Delta\Delta G_a$ | $\Delta\Delta G_a$ | $\Delta\Delta G_1$ |
| PM-Cys$_{27}$ | NA | NA | $-10.0 \pm 0.1$ | NA | NA | $-8.0 \pm 0.2$ | NA | NA | $+2.0 \pm 0.1^b$ |
| Tyr$_{139}$ | $-8.4 \pm 0.1$ | $-16.1 \pm 0.1$ | $-11.6 \pm 0.1$ | $-6.9 \pm 0.6$ | $-13.8 \pm 0.3$ | $-9.5 \pm 0.4$ | $+1.5 \pm 0.6^b$ | $+2.3 \pm 0.3^b$ | $+2.1 \pm 0.4^b$ |
| $\Delta G_{cooperative}$ | $-1.5 \pm 0.1$ | | NA | $-0.8 \pm 0.7$ | | NA | $0.7 \pm 0.7$ | | NA |

[a] Data for native CaM were fit to the equation:

$$Y_{CaM_{native}} = \left[ b\frac{K_a[Ca^{2+}]_{free} + 2K_b[Ca^{2+}]_{free}^2}{2(1 + K_a[Ca^{2+}]_{free}) + K_b[Ca^{2+}]_{free}^2} + (1 - b)\frac{K_1[Ca^{2+}]_{free}}{1 + K_1[Ca^{2+}]_{free}} \right]$$

as described in the legend to Figure 10. In the case of pyrenylmaleimide, $b = 0$. It is assumed in the case of tyrosine that the biphasic calcium dependence of the fluorescence signal is related to the ability of Tyr$_{139}$ to sense the association of calcium with both domains in CaM. The parameters associated with oxidatively modified CaM were recovered from a fit to the entire data set using eq 10 under Experimental Procedures. The cooperative free energy between the high-affinity class of calcium binding sites detected by Tyr$_{139}$ (i.e., association constants $K_a$ and $K_b$) is estimated as $\Delta G_{cooperative} = \Delta G_b - 2\Delta G_a - RT \ln(4)$, as previously discussed (Pedigo & Shea, 1995). Observed differences in binding energies were judged significant using the Student's *t*-test ($P < 0.05$). Errors were propagated (Bevington, 1969). [b] $P < 0.05$ using a Student's *t*-test.

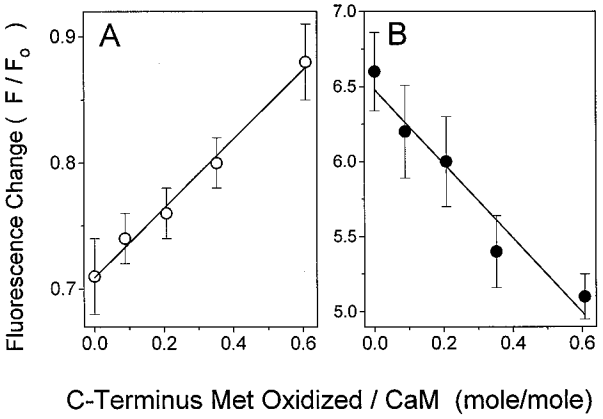


FIGURE 11: Fluorescence changes associated with target peptide binding to CaM. The steady-state change in fluorescence intensity ($F/F_0$) of pyrenylmaleimide-CaM (A) or Tyr$_{139}$ in CaM (B) associated with binding the MARCKS homolog (F52) peptide was measured subsequent to the oxidative modification of a variable number of methionines by $H_2O_2$ to the corresponding sulfoxide. $F_0$ and $F$ are the respective steady-state fluorescence intensities of CaM alone and in the presence of saturating concentrations of F52 peptide. In the case of pyrenylmaleimide-CaM, excitation was at 351 nm, and the fluorescence emission was collected subsequent to a Schott GG400 long-pass filter. In the case of Tyr$_{139}$ on CaM, excitation was at 275 nm, and the fluorescence emission was measured subsequent to a Oriel band-pass filter centered at 320 nm (full-width half-maximum is 10 nm). In all cases, the concentration of CaM was 0.26 $\mu$M, and peptide binding was measured in a buffer containing 0.1 M HEPES (pH 7.5), 0.1 M KCl, and 0.1 mM $CaCl_2$ at 25 °C. Errors represent the standard deviation of the mean for two separate measurements. The data were fit assuming a two-state model (eq 10) in which the observed fluorescence changes are assumed to be a linear combination of the associated fluorescence changes that decribe $CaM_{native}$ and $CaM_{oxidized}$. The associated amplitudes corresponding to the native and oxidatively modified populations of CaM were found to correspond closely with the extent of oxidative modification associated with the C-terminal vicinal methionines, and for reasons discussed in Figure 5 were held fixed in fitting the data shown in panels A and B. There was no apparent correlation with respect to the oxidative modification of methionines at other sites within CaM.

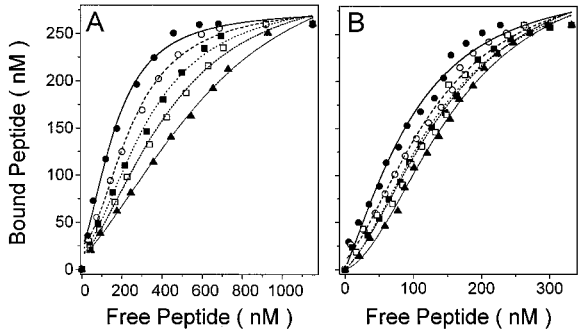


FIGURE 12: Titration of CaM with target peptides. Peptide binding of the MARCKS homolog (F52) or Ca-ATPase C25W peptide (measured only in panel A; data not shown) was measured as described under Experimental Procedures (eqs 8 and 9) using the fluorescence changes associated with peptide binding for both pyrenylmaleimide-labeled CaM (A) and the intrinsic fluorescence associated with Tyr$_{139}$ in CaM (B). Peptide binding is illustrated as a function of free peptide concentration for native CaM (●), and subsequent to the oxidative modification of 0.33 Met (○), 0.59 Met (■), 0.92 Met (□), and 1.27 Met (▲) to the corresponding sulfoxide, per CaM. Maximal fluorescent changes for native CaM correspond to a 29 ± 2% and 34 ± 3% decrease in the steady-state fluorescence intensity of pyrenylmaleimide associated with binding F52 and C25W, respectively (A). There is a 660 ± 30% increase in the steady-state fluorescence intensity of Tyr$_{139}$ associated with binding F52 (B). The data for native CaM were fit using eq 7. These values were held constant, and the individual data sets associated with PM and Tyr$_{139}$ were fit using eq 10. The associated binding energies for native and the oxidatively modified species of CaM are summarized in Table 5. In all cases, the concentration of CaM was 0.26 $\mu$M, and peptide binding was measured in a buffer containing 0.1 M HEPES (pH 7.5), 0.1 M KCl, and 0.1 mM $CaCl_2$ at 25 °C.

binding changes from 29 ± 3% in native CaM to 12 ± 3% upon the conversion of 1.3 ± 0.1 methionines per CaM to their corresponding sulfoxide. The change in tyrosine fluorescence associated with peptide binding changes from 660 ± 30% in native CaM to 510 ± 15% subsequent to the oxidation of 1.3 ± 0.1 methionines per CaM to their corresponding sulfoxide. This indicates that while the oxidatively modified CaM undergoes analogous structural changes upon calcium binding to native CaM (Figure 8), the oxidatively modified CaM binds to the target peptide in an altered conformation, such that changes in the environment of pyrenylmaleimide (at Cys$_{27}$) and Tyr$_{139}$ associated with peptide binding are reduced.

Using the fluorescence intensities of pyrenylmaleimide and tyrosine, we are able to assess the binding affinity between the amino and carboxyl domains of CaM and the target peptides (Figure 12; Table 5). It is apparent that the binding profile associated with Tyr$_{139}$ saturates at a lower concentration of free peptide than observed in the binding profile monitored with pyrenylmaleimide. This is consistent with previous measurements indicating that the C-terminal domain of CaM binds preferentially to a peptide sequence homolo-

Table 5: Free Energy Changes Associated with Peptide Binding to Calmodulin[a]

| | native calmodulin | | oxidized calmodulin | | difference (oxidized CaM − native CaM) | |
|---|---|---|---|---|---|---|
| reporter group | $\Delta G_1$ (kcal mol$^{-1}$ K$^{-1}$) | $\Delta G_2$ (kcal mole$^{-1}$ K$^{-1}$) | $\Delta G_1$ (kcal mol$^{-1}$ K$^{-1}$) | $\Delta G_2$ (kcal mol$^{-1}$ K$^{-1}$) | $\Delta\Delta G_1$ (kcal mol$^{-1}$ K$^{-1}$) | $\Delta\Delta G_2$ (kcal$^{-1}$ mol$^{-1}$ K$^{-1}$) |
| (A) calmodulin | | | | | | |
| PM-Cys$_{27}$ | $-8.6 \pm 0.5$ | $-9.7 \pm 0.5$ | $-7.1 \pm 0.2$ | $-10.3 \pm 0.1$ | $+1.5 \pm 0.5$[b] | $-0.6 \pm 0.5$ |
| Tyr$_{139}$ | $-9.2 \pm 0.1$ | $-9.5 \pm 0.3$ | $-8.0 \pm 0.2$ | $-10.5 \pm 0.2$ | $+1.2 \pm 0.2$[b] | $-1.0 \pm 0.4$[b] |
| average | $-8.9 \pm 0.4$ | $-9.6 \pm 0.1$ | $7.6 \pm 0.6$ | $-10.4 \pm 0.1$ | $+1.4 \pm 0.2$[b] | $-0.8 \pm 0.3$ |
| (B) target peptide | | | | | | |
| Trp$_4$ | $-5.9 \pm 2.8$ | $-12.9 \pm 2.8$ | $-6.0 \pm 3.5$ | $-13.3 \pm 3.5$ | $-0.1 \pm 4.5$ | $-0.4 \pm 4.5$ |

[a] Data were obtained from fits in Figures 12 and 13 to a Scatchard equation assuming two independent binding sites for target peptides per CaM and using eq 10 under Experimental Procedures, and the associated free energies are taken to be related to the association constants for each separate binding domain in CaM. Errors associated with each sample were propagated (Bevington, 1969), while average errors are the standard deviation of the measurement. [b] $P < 0.05$ using a Student's *t*-test.

gous to the autoinhibitory domain of the Ca-ATPase (Vorherr et al., 1990), since the placement of pyrenylmaleimide in the amino-terminal domain of CaM and Tyr$_{139}$ in the carboxyl-terminal domain would suggest that these fluorescent reporter groups preferentially monitor binding interactions associated with their respective globular domains within CaM.

In the case of the pyrene-labeled CaM, analogous binding curves are observed using both C25W and F52 (data not shown), suggesting that the association with these two target peptides occurs in an analogous manner. This is consistent with previous measurements that indicate a similar conformation of native CaM associated with these peptides, as assessed both by time-resolved fluorescence resonance energy transfer and by anisotropy measurements (Yao & Squier, 1994). A quantitative description of the binding interaction between CaM and these target peptides requires that we take into account both of the binding sites within CaM for target peptide (Table 5), as judged by our inability to adequately describe the data using equations that assume a single binding site (data not shown). We resolve two very similar binding constants associated with the interaction of CaM with the F52 target peptide irrespective of whether the binding is monitored using the signals from Tyr$_{139}$ or pyrenylmaleimide at Cys$_{27}$ (Table 5), suggesting that the environments around both Tyr$_{139}$ and pyrene located at Cys$_{27}$ are sensitive to peptide binding at the opposing globular domain. The latter result is consistent with the close proximity of the two globular domains subsequent to association with target peptides [reviewed by Crivici and Ikura (1995)]. The higher affinity of the carboxyl domain of CaM with target peptides suggests that the apparent binding energies between the amino and carboxyl domains of native CaM and F52 are $-8.9 \pm 0.4$ kcal mol$^{-1}$ K$^{-1}$ and $-9.6 \pm 0.1$ kcal mol$^{-1}$ K$^{-1}$, respectively. Using this assignment relating to the relative binding energies of the amino- and carboxyl-terminal domains of CaM and target peptides, we find that there is a loss of $1.4 \pm 0.2$ kcal mol$^{-1}$ K$^{-1}$ of binding energy between the amino-terminal domain of CaM and target peptide subsequent to the oxidative modification of the carboxyl-terminal vicinal methionines, while there is a $0.8 \pm 0.3$ kcal mol$^{-1}$ K$^{-1}$ enhancement in the affinity of the carboxyl-terminal domain of CaM with the associated binding site on the target peptide subsequent to the oxidative modification of the carboxyl-terminal vicinal methionines. This result is consistent with the interpretation that oxidatively modified CaM can associate with the PM-Ca-ATPase and function as a noncompetitive inhibitor.

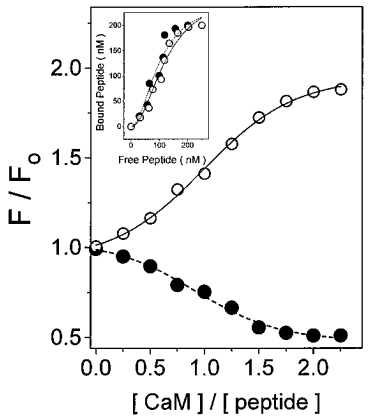


FIGURE 13: Peptide conformation in association with native and oxidatively modified CaM. The association of CaM with a peptide homologous to the autoinhibitory domain of the PM-Ca-ATPase (C25W) was monitored through changes in the initial fluorescence of Trp$_4$ located on the C25W peptide (i.e., $F/F_0$) upon association with native (○) and oxidatively modified (●) CaM. The latter sample involved the exposure of CaM to $H_2O_2$ for 10 h such that an average of $1.3 \pm 0.1$ methionines are oxidized to their corresponding sulfoxide per CaM (see Experimental Procedures). $F$ is the observed fluorescence signal, and $F_0$ is the initial fluorescence observed in the absence of added CaM. Maximal fluorescence changes correspond to an $88 \pm 6\%$ increase upon binding native CaM, and a $49 \pm 5\%$ decrease upon binding oxidatively modified CaM. Inset: Scatchard plot relating to peptide binding was analyzed as described in Figure 12. In all cases, the peptide concentration was 0.2 $\mu$M, and the buffer consisted of 0.1 M HEPES (pH 7.5), 0.1 M KCl, and 0.1 mM $CaCl_2$ at 25 °C.

*Peptide Conformation in Association with CaM.* In order to further investigate possible differences between the affinity and structure of native and oxidatively modified CaM in association with target peptides, we have further investigated the interaction of CaM with the C25W peptide. Binding was monitored through changes in the fluorescence of the single tryptophan located on the C25W peptide (i.e., Trp$_4$) using both native and oxidatively modified CaM (Figure 13). Trp$_4$ on the autoinhibitory domain of the PM-Ca-ATPase has previously been identified as a major hydrophobic anchor in the association of the homologous autoinhibitory domains from smooth and skeletal myosin light chain kinase [reviewed by Crivici and Ikura (1995)] and interacts with the carboxyl-terminal domain of peptides that are homologous to the autoinhibitory domain of the PM-Ca-ATPase (Chapman et al., 1992). This indicates that Trp$_4$ should serve as a sensitive probe to detect modifications in the interaction between target peptides and the carboxyl domain of CaM.

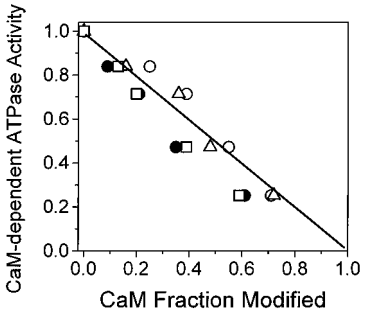


FIGURE 14: Correlation between CaM-dependent activation of PM-Ca-ATPase and fraction of CaM that is oxidatively modified. The ATPase activity is normalized to that obtained using native (unoxidized) CaM to activate the erythrocyte PM-Ca-ATPase, and the plotted values on the ordinate represent the average activation obtained from Figures 5 and 6 in which the CaM and calcium dependence of ATPase activity is assessed. The associated standard deviations for these measurements correspond to ±4% with respect to the ATPase activity. The associated values on the abscissa represent either direct measurements relating to the amount of T12 peptide that is oxidatively modified (●; obtained from Figure 3 with a standard error of ±6%) or the respective amplitudes obtained using the two-state model described under Experimental Procedures (eq 10) to obtain a consistent set of parameters that describe the oxidatively modified species of CaM. The latter data sets correspond to the associated amplitudes obtained from the four lifetime data sets in Figure 9 (○; with an associated standard error of 18%), the calcium-dependent titration of the steady-state fluorescence associated with both PM and $Tyr_{139}$ in Figure 10 (△; with an associated standard error of 12%), and the observed fluorescence change of both PM and $Tyr_{139}$ associated with peptide binding in Figure 11 (□; with an associated standard error of 7%). The line illustrates the expected relationship if there was a 1:1 correspondence between CaM-dependent ATPase activity and the fraction of CaM species that had been structurally modified subsequent to oxidative modification.

One observes that upon titration of the C25W peptide with native CaM that there is a 88 ± 6% fluorescence enhancement associated with the binding of CaM to C25W. In contrast to native CaM, one observes a 49 ± 5% decrease in the fluorescence associated with $Trp_4$ on C25W upon peptide association with oxidatively modified CaM (Figure 13), indicating an increased polarity surrounding $Trp_4$ (Schöneich et al., 1995). Given the critical role of the oxidatively sensitive C-terminal vicinal methionines (i.e., $Met_{146}$ and $Met_{147}$ in wheat germ CaM) in binding $Trp_4$ in a range of target peptides [reviewed by Crivici and Ikura (1995)], the altered polarity of $Trp_4$ upon association of the C25W peptide with oxidatively modified CaM indicates that $Trp_4$ in the C25W peptide associates with oxidatively modified CaM in an altered binding pocket. However, oxidative modification does not significantly alter the binding affinity between C25W and the carboxyl-terminal domain of the oxidatively modified CaM relative to native CaM (Table 5; Figure 13), consistent with our observation that oxidatively modified CaM can compete with native CaM for occupancy of the autoinhibitory domain on the PM-Ca-ATPase (Figures 5 and 6).

## DISCUSSION

It is widely recognized that the calcium handling capacity of a range of tissues including brain, heart, and erythrocytes isolated from aged animals declines, resulting in both longer calcium transients and elevated basal levels of intracellular calcium (Aiken et al., 1992; Michaelis, 1989; Michaelis et al., 1992; Peterson, 1992). Likewise, increased protein oxidation (and degradation) is observed in brain, heart, erythrocyte membranes, and various other tissues obtained from aged animals (Smith et al., 1991; Gaczynski, 1992), and it has been suggested that these processes are correlated (Harman, 1987). While age-dependent modifications in the calcium handling properties of the plasma membrane occur (Michaelis, 1989; Michaelis et al., 1992), there is no mechanistic information relating to the primary defect associated with the decline in transporter function. Likewise, specific decreases in the amount of CaM in aged brain have been reported [reviewed by Peterson (1992)], which may arise as a result of increased protein degradation. However, the identification of specific proteins that contain functionally relevant sites that are selectively damaged by ROS remains problematic.

Our approach to the identification of possible mechanisms relating to the decline in the calcium handling capabilities in cells that occurs in association with oxidative stress and aging has been to investigate the possibility that critical amino acids within CaM both are primary sites of oxidative modification and that upon oxidative modification alter the function of CaM. CaM was chosen as a possible target for oxidative modification (i) due to its key role in responding to and regulating intracellular calcium levels and (ii) because of its abnormally high methionine content, which comprises about 6% of the total amino acids in CaM. Since methionine is especially prone to oxidative modification (Vogt, 1995) and is critically involved in the association between CaM and target proteins (Meador et al., 1992, 1993; Ikura et al., 1992), it is expected that the conversion of this relatively hydrophobic amino acid to a polar residue would affect the function of CaM. We have emphasized conditions that maximize the specificity of oxidative modification to methionine by $H_2O_2$ (i.e., pH 5.0), in order to facilitate the identification of fundamental relationships between sites of oxidative modification and the underlying structural alterations that affect function. However, in order to generalize our results, we have considered both more physiological conditions using $H_2O_2$ (i.e., pH 7.5) and other more reactive species (i.e., peroxynitrite) which modify methionines within CaM on a subsecond time scale, and find nearly identical patterns of oxidative modification (Yin et al., 1995; Hühmer et al., 1995). In all cases, the same carboxyl-terminal methionines represent the primary sites of oxidative modification. We find that there is a close correlation with respect to the solvent accessibility of individual methionines and the extent to which methionine is oxidatively modified by $H_2O_2$ (Table 2, Figure 4). These results indicate that the pattern of modification is primarily determined by the solvent accessibilities of methionine to ROS, and suggest that results obtained from our more selective conditions (in which the modification of minor amounts of tyrosine, histidine, or lysine is prevented from complicating the interpretation of the functional and structural effects of oxidation; Toennies & Callan, 1939; Vogt, 1995) are generalizable to the consideration of the functional and structural effects relating to oxidative modification of CaM under physiological conditions.

*Summary of Results.* Reversed-phase HPLC and FAB mass spectrometry have allowed us to identify the existence of a highly reactive methionine near the carboxyl-terminal of CaM (i.e., $Met_{146}$ or $Met_{147}$ in wheat germ CaM), which represents the major site of oxidative modification by $H_2O_2$

(Figures 2 and 3). The selective oxidation of one of the carboxyl-terminal vicinal methionines to the corresponding sulfoxide results in a modified CaM that is unable to fully activate the PM-Ca-ATPase from erythrocyte membranes irrespective of the calcium concentration, or the CaM concentration used to assess function (Figures 5 and 6). There is a greater than 10-fold decrease in the calcium affinity for both amino- and carboxyl-terminal domains in CaM upon oxidative modification of a limited number of methionines (Table 4). The requirement for increased calcium concentrations to fully activate CaM is consistent with the observed increase in free calcium levels in cells that have undergone oxidative damage, since calcium extrusion requires activation of the PM-Ca-ATPase by calcium-saturated CaM [reviewed by Carafoli (1987) and Peterson (1992)]. However, while oxidative modification disrupts the tertiary structure of CaM, one observes analogous structural changes associated with the calcium activation of the individual globular domains, as indicated by the similar calcium-dependent changes in the fluorescence signals associated with $Tyr_{139}$ (carboxyl terminal) and pyrenylmaleimide (covalently linked to $Cys_{27}$ in the amino-terminal domain) (Figures 8 and 9). Subsequent to calcium activation, oxidatively modified CaM has an analogous affinity to the autoinhibitory domain of either a homolog of the MARCKS protein (i.e., F52) or the PM-Ca-ATPase (Figures 12 and 13), but upon binding is not able to activate the PM-Ca-ATPase (Figures 5 and 6). Since the oxidized CaM represents a mixed population of species, which includes significant levels of native CaM (even the most extensively oxidized sample contains an average of only $1.3 \pm 0.1$ methionines oxidized per CaM), the inability to regain maximal activation of the PM-Ca-ATPase upon addition of increasing concentrations of CaM indicates that the oxidatively modified CaM binds to the same site as native CaM, but with an altered conformation. This interpretation is consistent with our ability to describe the kinetic data in Figure 5 using a simple noncompetitive model relating to enzyme inhibition, in which oxidatively modified CaM is assumed to function as a noncompetitive inhibitor, and is further supported by the inability to recover maximal ATPase activity upon activation of the PM-Ca-ATPase in the presence of a mixture of oxidized and native CaM (1:10 stoichiometry; data not shown). However, the interaction between the autoinhibitory domain of the PM-Ca-ATPase and CaM is substantially different upon oxidative modification of CaM (Figure 13), as indicated by the opposing change in the fluorescence signal associated with $Trp_4$ in the target peptide upon binding to oxidatively modified CaM. However, there is no corresponding loss in binding energy between CaM and $Trp_4$ on the target peptide of C25W (Figure 13). Therefore, since the carboxyl-terminal methionines in CaM bind to $Trp_4$ in the target peptide (Chapman et al., 1992), and represent a major binding site that serves as a hydrophobic anchor with respect to the association of CaM and target peptides [reviewed by Crivici and Ikura (1995)], it is apparent that the altered fluorescence associated with $Trp_4$ in the target peptide upon association with oxidatively modified CaM is consistent with the association of $Trp_4$ on the target peptide with the corresponding methionine sulfoxides at the carboxyl terminus of CaM.

Quantitation of the binding interaction between CaM and target peptides indicates that oxidative modification of the carboxyl-terminal vicinal methionines results in the selective decrease in the association constant between one of the two domains of CaM and the target peptides (Figure 12, Table 5). Previous results indicate that the carboxyl-terminal domain of CaM both binds a peptide with sequence homology to the autoinhibitory domain of the PM-Ca-ATPase with higher affinity (Vorherr et al., 1990) and selectively associates with $Trp_4$ on the target peptide (Chapman et al., 1992). Therefore the greater than 7-fold reduction in the affinity of the peptide binding site on CaM that initially has lower affinity (Table 5) coupled with the fact that the binding energy between $Trp_4$ and the carboxyl terminus of CaM is not altered subsequent to the oxidative modification of CaM indicates that the loss of binding energy upon oxidative modification of methionines at the carboxyl terminus selectively alters the ability of the amino-terminal domain of CaM to bind to target peptides. These results indicate that oxidatively modified CaM is not able to activate the PM-Ca-ATPase as a result of the altered conformation associated with binding the autoinhibitory domain of the PM-Ca-ATPase.

*Correlation between the CaM-Dependent ATPase Activity of the PM-Ca-ATPase and the Oxidative Modification of the Carboxyl-Terminal Vicinal Methionines in CaM.* Possible correlations between the decrease in the CaM-dependent ATPase activity (Figures 4 and 5), the oxidative modification of the carboxyl-terminal vicinal methionines (Figures 2 and 3; Tables 2 and 3), and perturbations to CaM's structure were assessed through a comparison of the relative amplitudes associated with the recovered parameters relating to oxidatively modified CaM that were generated using a two-state model. This model assumes that the distribution of species associated with oxidatively modified CaM can be approximated by two populations: (i) oxidatively modified CaM with native-like structure and (ii) oxidatively modified CaM with an altered tertiary structure. We find that there is a good correlation between the loss of the CaM-dependent ATPase activity associated with the oxidative modification of the carboxyl-terminal vicinal methionines and the amplitudes associated with (i) the modification of the lifetimes of pyrene (covalently linked to $Cys_{27}$) and $Tyr_{139}$ (Figure 9), (ii) the decreased calcium affinity of CaM assessed by calcium-dependent changes in the fluorescence of pyrene and $Tyr_{139}$ (Figure 10), and (iii) the observed fluorescence change of both pyrene and $Tyr_{139}$ associated with peptide binding (Figure 11). This correlation is illustrated in Figure 14, and provides strong support that the carboxyl-terminal vicinal methionines represent a regulatory site on CaM that modulates CaM's ability to productively associate with and activate the PM-Ca-ATPase.

*Relationship to Other Work.* Relatively little information is available with respect to the relationship between oxidative damage to CaM and its ability to regulate target proteins. It has been previously observed that the oxidation of three to four methionines in animal CaM (localized primarily in the central helix and calcium binding domains III and IV) with *N*-chlorosuccinimide and chloramine T results in a *gradual* decrease in the ability of CaM to activate (i) cyclic nucleotide phosphodiesterase, (ii) adenylate cyclase, and (iii) the erythrocyte Ca-ATPase [Walsh & Stevens, 1977; Wolff et al., 1980; Guerini et al., 1987; reviewed by Carafoli et al. (1988)]. Whereas Walsh and Stevens (1977) found that residues $Met_{71}$, $Met_{72}$, $Met_{76}$, and possibly $Met_{109}$ were predominantly affected, Guerini et al. (1987) arrived at the conclusion that the oxidized methionine residues are located

within the carboxyl-terminal half of the protein and might also include $Met_{124}$, $Met_{144}$, and $Met_{145}$. The oxidized protein was ineffective in binding to cyclic nucleotide phosphodiesterase. These results provided the first suggestion that methionine residues in CaM play a critical role in modulating CaM's ability to activate target proteins, and suggest that oxidative modification to CaM results in a population of modified CaMs that is unable to bind to target proteins. However, these results do not address the influence of more selective oxidative modifications with respect to the ability of CaM to bind and activate target proteins.

*Role of Methionine Residues in Binding Target Proteins.* Calcium activation of CaM results in structural rearrangements that expose two hydrophobic patches that are enriched in methionine residues, which forms as much as 46% of the binding surface for target proteins (O'Neil & DeGrado, 1990). The unique role of methionine in forming a hydrophobic binding site that displays minimal steric requirements and can therefore more rapidly bind target proteins has been highlighted as critical to CaM's ability to act as a signal transduction molecule (Gellman, 1991; Williams, 1992; Clore et al., 1993). Furthermore, it has been demonstrated that the vicinal methionines near the carboxyl-terminal domain of CaM are critical in defining one of two major hydrophobic anchors that selectively associate with the target peptide (at a site analogous to $Trp_4$ in both smooth and skeletal myosin light chain kinase; Crivici & Ikura, 1995). While it is generally thought that conservative substitutions at this site have a relatively modest effect on CaM's function (Zhang et al., 1994), Kung and co-workers have identified a conservative substitution within CaM of $Val_{145}$ for $Met_{145}$ that is associated with a behavioral mutant in paramecium (Kink et al., 1990). The subsequent characterization of this mutant CaM indicated that it does not fully support the activation of selected target proteins (i.e., the calcium-dependent potassium current), emphasizing the importance of $Met_{145}$ in correctly binding and activating some target proteins [reviewed by Kung et al. (1992)].

*Physiological Significance of Oxidative Modification of Methionine by $H_2O_2$.* The oxidation of methionine by $H_2O_2$ is of particular interest, since $H_2O_2$ represents the most abundant ROS normally produced during cellular metabolism, and contributes to a range of chronic conditions associated with oxidative stress (Smith et al., 1991; Kukreja & Hess, 1992, 1994; Warner, 1994). While the oxidative modification of methionine is relatively slow (Figure 2), average cellular concentrations of $H_2O_2$ can exceed 100 $\mu$M for extended periods of time (i.e., $\sim$1 h) during ischemia and reperfusion in rat striatum (Hyslop et al., 1995), and localized concentrations of $H_2O_2$ may reach the millimolar concentration ranges used in this study. Furthermore, peroxides have been suggested to specifically target the calcium regulatory proteins and to interfere with signal transduction in a range of cell types under conditions of oxidative stress (Chaudière, 1994). For example, following ischemic conditions large concentrations of MetSO have been detected in cardiac tissue (Fliss & Docherty, 1987), indicating that oxidative modification of methionines is physiologically significant.

*Regulatory Role for Oxidatively Sensitive Vicinal Methionines on CaM.* $H_2O_2$ (and other more reactive species such as peroxynitrite) as well as other oxidants (i.e., *N*-chlorosuccinimide, chloramine-T, and benzophenone) demonstrates a selectivity for the oxidative modification of the carboxyl-terminal vicinal methionines in CaM (Walsh & Stevens, 1977; O'Neil et al., 1989; Yin et al., 1995; Hühmer et al., 1995), suggesting that the structural and functional modifications to CaM resulting from the selective conditions used in this study to estimate the sensitivity of individual amino acids within CaM to oxidative modification by $H_2O_2$ have more general significance. Additional measurements involving the addition of iron to facilitate Fenton chemistry (i.e., the production of hydroxyl radicals at metal binding sites in the presence of $H_2O_2$; Stadtman, 1993) indicate a very similar oxidation pattern (data not shown), suggesting either that there are no metal binding sites for iron on CaM or that the lower oxidation potential or enhanced solvent accessibility of the C-terminal vicinal methionines functions to facilitate their selective oxidative modification by the highly reactive hydroxyl radical.

The ability to couple the oxidative modification of a single site (i.e., the carboxyl-terminal vicinal methionines which are conserved between all CaM's from higher plants to humans) on a regulatory protein such as CaM to the reduction of ATP utilization and energy metabolism within the cell has the potential to enhance cell viability during conditions of oxidative stress, and is relevant to a range of acute trama (e.g., head injury) in which ATP utilization and energy metabolism are rapidly shut down (Pazdernik et al., 1994). The evolutionary conservation of a site (i.e., the carboxyl-terminal vicinal methionines) that (i) has a lower oxidation potential with respect to oxidative modification and (ii) when oxidized modifies the association between CaM and target proteins so as to block activation by CaM suggests that this site may represent a regulatory site. We propose that the inactivation of CaM by ROS can explain both the decline in energy metabolism (and the associated decline in ATP levels) and the rise in intracellular calcium levels identified with oxidative stress, and has the potential to enhance cell viability under conditions of oxidative stress. The decline in ATP content could arise from inactivation of a number of the over 30 critical (CaM-regulated) proteins involved in energy metabolism (e.g., glycogen phosphorylase), which would have the effect of reducing the flux of metabolites through the mitochondrial electron transport chain and the associated production of ROS. The associated increase in intracellular calcium levels is proposed to be the result of (i) a decline in ATP levels, resulting in decreased activity of the ATP-driven calcium pumps, and (ii) the inactivation of the CaM-dependent PM-Ca-ATPase by the association of oxidatively modified CaM with the autoregulatory domain (see above). This model proposes that the loss of calcium homeostasis and the decrease in intracellular ATP levels associated with oxidative stress represent an adaptive strategy of the cell to (i) decrease the production of ROS by shutting down oxidative metabolism and (ii) decrease ATP hydrolysis by the CaM-dependent ATPases in order to prevent the irreversible deamidation of adenosine to inosine, which can result in long-term energy depletion of the cell (Katz, 1992). Since oxidative stress involves the competition between oxidative damage and cellular repair mechanisms, a reduction in the concentration of ROS permits CaM to be repaired (by, for example, the methionine reductases; Brot & Weissbach, 1982, 1983, 1991; Rahman et al., 1992; Vogt, 1995), resulting in normal energy metabolism and normal intracellular calcium levels. This type of regulation by ROS would

correspond to a previously unrecognized level of control that could serve as a protective role against the cytotoxicity associated with oxidative stress.

*Conclusions.* The oxidative modification of one of the carboxyl-terminal vicinal methionines within CaM functions as a molecular switch to modify the binding mechanism of CaM with the PM-Ca-ATPase. Oxidatively modified CaM associates with the autoinhibitory peptide on the PM-Ca-ATPase, but does not activate the PM-Ca-ATPase. The decreased calcium affinity of oxidized CaM likewise has the potential to result in elevation of intracellular calcium levels, which is associated with oxidative stress in a range of cell types including brain and heart (Orrenius, 1990; Peterson, 1992; Smith et al., 1992). Therefore, the selective oxidation of CaM has the potential to modify calcium homeostasis within the cell.

## ACKNOWLEDGMENT

We are grateful for the many helpful discussions provided by Diana Bigelow, Ron Borchardt, Dick Himes, David Johnson, Eli Michaelis, Fred Sampson, and George Wilson. We thank David Johnson for providing the F52 peptide used in this study. We thank our reviewers for many helpful criticisms.

## REFERENCES

Aiken, N. R., Satterlee, J. D., & Galey, W. R. (1992) *Biochim. Biophys. Acta 1136*, 155−160.
Babu, Y. S., Sack, J. S., Greenough, T. J., Bugg, C. E., Means, A. R., & Cook, W. J. (1985) *Nature 315*, 37−40.
Babu, Y. S., Bugg, C. E., & Cook, W. J. (1988) *J. Mol. Biol. 204*, 191−204.
Barbato, G., Ikura, M., Kay, L. E., Pastor, R. W., & Bax, A. (1992)-*Biochemistry 31*, 5269−5278.
Beaudet, R., Saheb, S. A., & Drapeau, G. R. (1974) *J. Biol. Chem. 249*, 6468−6471.
Bevington, P. R. (1969) *Data Reduction and Error Analysis for the Physical Sciences*, McGraw-Hill, New York.
Blackshear, P. J. (1993) *J. Biol. Chem. 268*, 1501−1504.
Blackshear, P. J., Verghese, G. M., Johnson, J. D., Haupt, D. M., & Stumpo, D. J. (1992) *J. Biol. Chem. 267*, 13540−13546.
Brot, N., & Weissbach, H. (1982) *Trends Biochem. Sci. 7*, 137−139.
Brot, N., & Weissbach, H. (1983) *Arch. Biochem. Biophys. 223*, 271−281.
Brot, N., & Weissbach, H. (1991) *Biofactors 3*, 91−96.
Bruccoleri, B. R., & Karplus, M. (1986) *J. Comput. Chem. 7*, 165−175.
Burgess, W. H., Jemiolo, D. K., & Kretsinger, R. H. (1980) *Biochim. Biophys. Acta 623*, 257−270.
Carafoli, E. (1987) *Annu. Rev. Biochem., 56*, 395−433.
Carafoli, E. (1991) *Physiol. Rev. 71*, 129−153.
Carafoli, E., Krebs, J., & Chiesi, M. (1988) in *Calmodulin* (Cohen, P., & Klee, C. B., Eds.) pp 297−312, Elsevier, New York.
Cavieres, J. D. (1984) *Biochim. Biophys. Acta 771*, 241−244.
Chapman, E. R., Alexander, K., Vorherr, T., Carafoli, E., & Storm, D. R. (1992) *Biochemistry 31*, 12819−12825.
Chattopadhyaya, R., Meador, W. E., Means, A. R., & Quiocho, F. A. (1992) *J. Mol. Biol. 228*, 1177−1192.
Chaudière, J. (1994) in *Free Radical Damage and its Control* (Rice-Evans, C. A., & Burdon, R. H., Eds.) pp 25−66, Elsevier, New York.
Clark, M. R. (1988) *Physiol. Rev. 68*, 503−554.
Clark, M. R., & Shohet, S. B. (1985) *Clin. Haematol. 14*, 223−257.
Clore, G. M., Bax, A., Ikura, M., & Gronenborn, A. M. (1993) *Curr. Opin. Struct. Biol. 3*, 838−845.
Coyle, J. T., & Puttfarcken, P. (1993) *Science 262*, 689−695.
Crivici, A., & Ikura, M. (1995) *Annu. Rev. Biophys. Biomol. Struct. 24*, 85−116.
Fabiato, A. (1988) *Methods Enzymol. 157*, 378−417.
Fabiato, A., & Fabiato, F. (1979) *J. Physiol. Paris 75*, 463−505.
Falchetto, R., Vorherr, T., Brunner, T., & Carafoli, E. (1991) *J. Biol. Chem. 266*, 2930−2936.
Falick, A. M., & Maltby, D. A. (1989) *Anal. Biochem. 182*, 165−169.
Fliss, H., & Docherty, G. (1987) *Dev. Cardiovasc. Med. 67*, 85−98.
Gaczynski, M. (1992) *Cytobios 72*, 290−291.
Gellman, S. H. (1991) *Biochemistry 30*, 6633−6636.
Glass, R. S. (1990) in *Sulfur-Centered Reactive Intermediates in Chemistry and Biology* (Chatgilialoglu, C., & Asmus, K.-D., Eds.) pp 213−226, Plenum Press, New York.
Gornal, A., Bardawill, C., & David, M. (1949) *J. Biol. Chem. 177*, 751−766.
Guerini, D., Krebs, J., & Carafoli, E. (1987) *Eur. J. Biochem. 170*, 35−42.
Harman, D. (1987) in *Modern Biological Theories of Aging* (Butler, R. N., Schneider, E. L., Sprott, R. L., & Warner, H. R., Eds) pp 81−87, Raven Press, New York.
Haugland, R. P. (1992) *Handbook of Fluorescent Probes and Research Chemicals*, 5th ed., Molecular Probes, Inc., Eugene, OR.
Hinds, T. R., & Andreasen, T. J. (1981) *J. Biol. Chem. 256*, 7877−7881.
Hühmer, A. F. R., Gerber, N. C., Ortiz de Montellano, P. R., & Schöneich, Ch. (1995) submitted to *Chem. Res. Toxicol.* (submitted for publication).
Hyslop, P. A., Zhang, Z., Pearson, D. V., & Phebus, L. A. (1995) *Brain Res. 671*, 181−186.
Ikura, M., Hiraoki, M., Mikuni, T., Yazawa, M., & Yagi, K. (1983)-*Biochemistry 22*, 2573−2579.
Ikura, M., Kays, L. E., Krinks, M., & Bax, A. (1991) *Biochemistry 30*, 5498−5504.
Ikura, M., Clore, G. M., Gronenborn, A. M., Zhu, G., Klee, C. B., & Bax, A. (1992) *Science 256*, 632−638.
Johnson, J. D. (1983) *Biochem. Biophys. Res. Commun. 112*, 787−793.
Johnson, M. L., & Faunt, L. M. (1992) *Methods Enzymol. 210*, 1−37.
Katz, A. M. (1992) *Physiology of the Heart*, pp 633−634, 2nd ed., Raven Press, New York,
Kilhoffer, M.-C., Kubina, M., Travers, F., & Haiech, J. (1992) *Biochemistry 31*, 8098−8106.
Kink, J. A., Maley, M. E., Preston, R. R., et al. (1990) *Cell 62*, 165−174.
Klee, C. B. (1977) *Biochemistry 16*, 1017−1024.
Klee, C. B., & Vanaman, T. C. (1982) *Adv. Protein Chem. 35*, 213−321.
Klee, C. B., Crouch, T. H., & Krinks, M. H. (1979) *Proc. Natl. Acad. Sci. U. S. A. 76*, 6270−6273.
Kosk-Kosicka, D., Bzdega, T., & Johnson, J. D. (1990) *Biochemistry 29*, 1875−1879.
Kraulis, P. J. (1991) *J. Appl. Crystallogr. 24*, 946−950.
Kretsinger, R. H. (1992a) *Cell Calcium 13*, 363−376.
Kretsinger, R. H. (1992b) *Science 258*, 50−51.
Kukreja, R. C., & Hess, M. L. (1992) *Cardiovasc. Res. 26*, 641−655.
Kukreja, R. C., & Hess, M. L. (1994) *Free Radicals, Cardiovascular Dysfunction and Protective Strategies*, R. G. Landes Co., Austin, TX.
Kung, C., Preston, R. R., Maley, M. E., Ling, K.-Y., Kanabrocki, J. A., Seavey, B. R., & Saimi, Y. (1992) *Cell Calcium 13*, 413−425.
Kyte, J., & Doolittle, R. F. (1982) *J. Mol. Biol. 157*, 105−132.
Laemmli, U. K. (1970) *Nature 227*, 680−685.
Lakowicz, J. R. (1983) *Principles of Fluorescence Spectroscopy*, Plenum Publishing Corp., New York.
Lanzetta, P. A., Alverez, L. J., Reinsch, P. S., & Candia, O. (1979)-*Anal. Biochem. 100*, 95−97.
Levine, I. N. (1978) *Physical Chemistry*, McGraw Hill, Inc., New York.
Luedtke, R., Owen, C. S., Vanderkooi, J. M., & Karush, F. (1981) *Biochemistry 20*, 2927−2936.

MacKall, J., & Klee, C. B. (1991) *Biochemistry 30*, 7242−7247.
Manning, M. C., Patel, K., & Borchardt, R. T. (1989) *Pharm. Res. 6*, 903−918.
Matthews, J. C. (1993) *Fundamentals of Receptor, Enzyme, and Transport Kinetics*, CRC Press, Boca Raton.
Maune, J. F., Klee, C. B., & Beckingham, K. (1992) *J. Biol. Chem. 267*, 5286−5295.
Meador, W. E., Means, A. R., & Quiocho, F. A. (1992) *Science 257*, 1251−1255.
Meador, W. E., Means, A. R., & Quiocho, F. A. (1993) *Science 262*, 1718−1721.
Michaelis, M. L. (1989) *Ann. N.Y. Acad. Sci. 568*, 89−94.
Michaelis, M. L., Foster, C. T., & Jayawickreme, C. (1992) *Mech. Ageing Dev. 62*, 291−306.
Nelson, D. P., & Kiesow, L. A. (1972) *Anal. Biochem. 49*, 474−478.
Nicotera, P., Kass, G. E. N., Duddy, S. K., & Orrenius, S. (1991) in *Calcium, Oxygen Radicals and Cellular Damage* (Duncan, C. J., Ed.) pp 17−33, Cambridge University Press, New York.
Niggli, V., Penniston, J. T., & Carafoli, E. (1979) *J. Biol. Chem. 254*, 9955−9958.
Oliyai, C., Schöneich, Ch., Wilson, G., & Borchardt, R. (1992) in *Topics in Pharmaceutical Sciences 1991* (Crommelin, D. J. A., & Midha, K. K., Eds.) pp 23−46, Medical Pharm. Publishers, Stuttgart.
O'Neil, K. T., & DeGrado, W. F. (1990) *Trends Biochem. Sci. 15*, 59−64.
O'Neil, K. T., Erickson-Viitanen, S., & DeGrado, W. F. (1989) *J. Biol. Chem. 264*, 14571−14578.
Orrenius, S. (1990) in *Free Radicals, Lipoproteins, and Membrane Lipids* (de Paulet, C., Ed.) pp 257−267, Plenum Press, New York.
Ota, I. M., & Clark, S. (1989) *J. Biol. Chem. 264*, 54−60.
Patel, K., & Borchardt, R. T. (1990) *J. Parenter. Sci. Technol. 44*, 300−301.
Pazdernik, T., Cross, R., Nelson, S., Kamijo, Y., & Samson, F. (1994) *Neurochem. Res. 19*, 1393−1400.
Pedigo, S., & Shea, M. A. (1995) *Biochemistry 34*, 1179−1196.
Peterson, C. (1992) *Ann. N.Y. Acad. Sci. 663*, 279−293.
Potter, S. M., Henzel, W. J., & Aswad, D. W. (1993) *Protein Sci. 2*, 1648−1663.
Press, W. H., Flannery, B. P., Teukolsky, S. A., & Vetterling, W. T. (1988) *Numerical Recipes in C, The Art of Scientific Computing*, Cambridge University Press, New York.
Rahman, M. A., Nelson, H., Weissbach, H., & Brot, N. (1992) *J. Biol. Chem. 267*, 15549−15551.
Rao, S. T., Wu, S., Satyshur, K. A., Ling, K.-Y., Kung, C., & Sundaralingam, M. (1993) *Protein Sci. 2*, 436−447.
Rohlf, F. J., & Sokal, R. R. (1995) *Statistical Tables, 3rd ed.*, W. H. Freeman and Co., New York.
Rosen, D. R., Siddeque, T., Patterson, D., Figlewicz, D. A., Sapp, P., Hentati, A., Donaldson, D., Goto, J., O'Regan, J. P., Deng, H.-X., Rahman, Z., Krizus, A., McKenna-Yasek, D., Cayabyab, A., Gaston, S. M., Berger, R., Tanzi, R. E., Halperin, J. J., Herzfeldt, B., Van den Bergh, R., Hung, W.-Y., Bird, T., Deng, G., Mulder, D. W., Smyth, C., Laing, N. G., Sorianao, E., Pericak-Vance, A., Haines, J., Rouleau, G. A., Gusella, J. S., Horvitz, H. R., & Brown, R. H. (1993) *Nature 362*, 59−62.
Royer, C. A. (1993) *Biophys. J. 65*, 9−10.
Sanaullah, Wilson, G. S., & Glass, R. S. (1994) *J. Inorg. Biochem. 55*, 87−99.
Schöneich, Ch., Hühmer, A. F. R., Rabel, S. R., Stobaugh, J. F., Jois, S. D. S., Larive, C. K., Siahaan, T. J., Squier, T. C., Bigelow, D. J., & Williams, T. D. (1995) *Anal. Chem. 67*, 155R-181R.
Seamon, K. B. (1980) *Biochemistry 19*, 207−215.
Smith, C. D., Carney, J. M., Tatsumo, T., Stadtman, E. R., Floyd, R. A., & Markesbery, W. R. (1992) *Ann. N.Y. Acad. Sci. 663*, 111−119.
Stadtman, E. R. (1992) *Science 257*, 1220−1224.
Stadtman, E. R. (1993) *Annu. Rev. Biochem. 62*, 797−821.
Strasburg, G. M., Hogan, M., Birmachu, W., Thomas, D. D., & Louis, C. F. (1988) *J. Biol. Chem. 263*, 542−548.
Takemoto, L., & Emmons, T. (1991) *Curr. Eye Res. 10*, 865−869.
Thulin, E., Andersson, A., Drakenberg, T., Forsen, S., & Vogel, H. J. (1984) *Biochemistry 23*, 1862−1870.
Toda, H., Yazawa, M., Sakiyama, F., & Yagi, K. (1985) *J. Biochem. (Tokyo) 98*, 833−842.
Toennies, G., & Callan, T. P. (1939) *J. Biol. Chem. 139*, 481−490.
Török, K., Lane, A. N., Martin, S. N., Janot, J.-M., & Bailey, P. M. (1992) *Biochemistry 31*, 3452−3462.
Trewhella, J., Liddle, W. K., Heidorn, D. B., & Strynadka, N. (1989) *Biochemistry 28*, 1294−1300.
Trybus, K. M., & Lowey, S. (1985) *J. Biol. Chem. 260*, 15988−15995.
Vogt, W. (1995) *Free Radicals Biol. Med. 18*, 93−105.
Vorherr, T., James, P., Krebs, J., Enyedi, A., McCormick, D. J., Penniston, J. T., & Carafoli, E. (1990) *Biochemistry 29*, 355−365.
Vorherr, T., Kessler, T., Hofman, F., & Carafoli, E. (1991) *J. Biol. Chem. 266*, 22−27.
Walsh, M., & Stevens, F. C. (1977) *Biochemistry 16*, 2742−2749.
Wang, C.-L. A. (1989) *Biochemistry 28*, 4816−4820.
Wang, C.-L. A., Aquaron, R. R., Leavis, P. C., & Gergely, J. (1982) *Eur. J. Biochem. 124*, 7−12.
Wang, C.-L. A., Leavis, P. C., & Gergely, J. (1984) *Biochemistry 23*, 6410−6415.
Warner, H. R. (1994) *Free Radicals Biol. Med. 17*, 249−258.
Williams, R. J. P. (1992) *Cell Calcium 13*, 355−362.
Wolff, J., Cook, G. H., Goldhammer, A. R., & Berkowitz, S. A. (1980) *Proc. Natl. Acad. Sci. U.S.A. 77*, 3841−3844.
Wylie, D. C., & Vanaman, T. C. (1988) in *Calmodulin* (Cohen, P., & Klee, C. B., Eds.) pp 1−15, Elsevier, New York.
Yao, Y., & Squier, T. C. (1994) *Biophys. J. 66*, A73.
Yao, Y., Schöneich, Ch., & Squier, T. C. (1994) *Biochemistry 33*, 7797−7810.
Yazawa, M., Matsuzawa, F., & Yagi, K. (1990) *J. Biochem. (Tokyo) 107*, 287−291.
Yin, D., Hühmer, A., Schöneich, Ch., & Squier, T. C. (1995) *Biophys. J. 68*, A165.
Yoshida, M., Minowa, O., & Yagi, K. (1983) *J. Biochem. (Tokyo) 94*, 1925−1933.
Zhang, M., Li, M., Wang, J. H., & Vogel, H. J. (1994) *J. Biol. Chem. 269*, 15546−15552.

BI951712I